Developmental Biology 410 (2016) 135–149

Contents lists available at ScienceDirect

Developmental Biology

journal homepage: www.elsevier.com/locate/developmentalbiology

The adaptor protein Cindr regulates JNK activity to maintain epithelial sheet integrity

Hannah W.R. Yasin [1], Samuel H. van Rensburg [1], Christina E. Feiler [1,2], Ruth I. Johnson *

Biology Department, Wesleyan University, 52 Lawn Avenue, Middletown, CT, USA

ARTICLE INFO

Article history:
Received 1 September 2015
Received in revised form
23 December 2015
Accepted 4 January 2016
Available online 7 January 2016

Keywords:
Cindr
Cd2ap
Cin85
JNK
Epithelial integrity

ABSTRACT

Epithelia are essential barrier tissues that must be appropriately maintained for their correct function. To achieve this a plethora of protein interactions regulate epithelial cell number, structure and adhesion, and differentiation. Here we show that Cindr (the *Drosophila* Cin85 and Cd2ap ortholog) is required to maintain epithelial integrity. Reducing Cindr triggered cell delamination and movement. Most delaminating cells died. These behaviors were consistent with JNK activation previously associated with loss of epithelial integrity in response to ectopic oncogene activity. We confirmed a novel interaction between Cindr and *Drosophila* JNK (dJNK), which when perturbed caused inappropriate JNK signaling. Genetically reducing JNK signaling activity suppressed the effects of reducing Cindr. Furthermore, ectopic JNK signaling phenocopied loss of Cindr and was partially rescued by concomitant *cindr* over-expression. Thus, correct Cindr-dJNK stoichiometry is essential to maintain epithelial integrity and disturbing this balance may contribute to the pathogenesis of disease states, including cancer.

1. Introduction

Multicellular organisms depend on epithelia for diverse functions including protection, compartmentalization of physiological systems, selective absorption, secretion and sensory reception. Given the importance of these functions, it is essential to better understand the mechanisms and molecules that, together, maintain the strength and integrity of epithelia. Diverse epithelia are assembled according to a similar plan: they typically consist of closely adherent polarized cells with simple shapes and at least one layer of cells closely associated with a basement membrane (Rodriguez-Boulan and Macara, 2014). Disrupting the internal organization of epithelial cells or their organization within the tissue can compromise the function of the epithelium. In addition the majority of fatal cancers are of epithelial origin (Weinberg, 2013). This is in part due to their exposure to carcinogens that can cause genetic mutations and because most epithelia retain mitotic potential to facilitate their rapid repair. If oncogenic mutations occur that deregulate proliferation, disrupt cell death and compromise cell polarity or adhesion, tumors and even metastases can occur (Halaoui and McCaffrey, 2015; Hanahan and Weinberg, 2011; Chaffer and Weinberg, 2011; Wogan et al., 2004; Martin-Belmonte and Perez-Moreno, 2012). A better understanding of how epithelia are maintained and regulated is therefore a priority.

Here we describe a role for the cytoplasmic *Drosophila* adaptor protein Cindr in maintaining the integrity of a pseudostratified epithelium, the fly wing. Cindr and its vertebrate orthologs Cd2ap and Cin85 contain multiple SH3 domains and several other protein interaction motifs that confer the ability to assemble multi-protein complexes that mediate diverse yet critical functions. Cindr and Cd2ap have previously been implicated in regulating the cytoskeleton and promoting stable cell adhesion via interactions with actin, the actin capping proteins (CPs), and GTPase activating proteins (GAPs) that target Arf6 and Cdc42 (Johnson et al., 2008, 2011, 2012; Faul et al., 2007; Bruck et al., 2006; Tang and Brieher, 2013; Zhao et al., 2013; Elbediwy et al., 2012; Yaddanapudi et al., 2011; Welsch et al., 2005; Mustonen et al., 2005; Lehtonen et al., 2002). Additionally an interaction between Cindr and Anillin at the cleavage furrow of mitotic cells is critical for cell proliferation (Haglund et al., 2010). In contrast the complexes assembled by Cin85 have mainly been implicated in regulating ubquitination and endocytosis of receptor tyrosine kinases (RTK) (Dikic, 2002,

List of abbreviations: CP, actin-capping protein; AJ, adherens junction; APF, after puparium formation; A/P, anterior/posterior; Bsk, basket; β-Gal, β-Galactosidase; JNK, c-Jun N-terminal kinase; Chic, chickadee; Dcr-2, dicer-2; D/V, dorsal/ventral; dJNK, Drosophila JNK; Jra or dJun, Drosophila Jun; Ecad, ecadherin; GMA, GFP: moesin-Actin-binding-domain; GFP, green fluorescent protein; GAPs, GTPase activating proteins; Hid, hid involution defective; MMP, matrixmetalloprotease; Ptc, patched; Puc, puckered; RTK, receptor tyrosine kinase; Slpr, slipper; TdT, terminal deoxynucleotidyl transferase; TUNEL, mediated dUTP nick end labeling; ZA, zonula adherens

* Corresponding author.
E-mail address: rijohnson@wesleyan.edu (R.I. Johnson).
[1] These authors contributed equally to this work.
[2] Present address: Center of Plant Molecular Biology, Eberhard-Karls-University of Tuebingen, Auf der Morgenstelle 32, Tuebingen, Germany.

http://dx.doi.org/10.1016/j.ydbio.2016.01.003
0012-1606/

2003) as well as adhesion proteins of the slit diaphragm, a specialized junction of the vertebrate kidney (Tossidou et al., 2010). When, where and how Cindr, Cd2ap and Cin85 assemble appropriate protein complexes to accomplish these diverse functions remains a challenge. Genetically tractable *Drosophila* tissues serve as models to examine the nature and function of these complexes and address these challenges.

In exploring how Cindr maintains the integrity of the fly wing epithelium, we uncovered novel interactions with JNK (c-Jun N-terminal kinase) signaling. We found that reducing Cindr in the developing wing epithelium caused dramatic cell delamination: some cells migrated short distances and many cells died. These cell behaviors were mediated in part by ectopic JNK signaling that was triggered in cells with lower concentrations of Cindr. JNK signaling is a critical kinase cascade that responds to a variety of stimuli including DNA damage, environmental stress, wounding and Tumor Necrosis Factor-α (Adler et al., 1995; Rosette and Karin, 1996; Ramet et al., 2002; Igaki et al., 2002; Moreno et al., 2002). Appropriate responses to these stimuli include apoptosis, cell migration and even cell proliferation, effects that are mediated by expression of an array of genes targeted by transcription factors including c-Jun and c-Fos, which in turn are activated by JNK (Picco et al., 2013; Stronach, 2005; Rios-Barrera and Riesgo-Escovar, 2012).

The relationship between JNK activity and the maintenance of epithelial integrity is complex. JNK drives cytoskeletal changes and migratory cell behaviors necessary to repair epithelial wounds (Rios-Barrera and Riesgo-Escovar, 2012; Repiso et al., 2011). Here we show that this JNK function contributes to the movement of cells that lack Cindr. In addition, JNK is an important antagonist of stable epithelial junctions (You et al., 2013). A fundamental feature of epithelia is the presence of apical AJs that are generated by homophilic interactions between epithelial cadherin (Ecad) dimers of adjacent cells (Harris and Tepass, 2010). The intracellular domains of Ecad interact with proteins at the plasma membrane including Catenins that provide links to the actin cytoskeleton. Extracellular interactions between apposing Ecad molecules and internal interactions with the cytoskeleton provide mechanical strength critical for epithelial integrity and support epithelial cell structure (Baum and Georgiou, 2011). However, activated JNK leaves AJs susceptible to disassembly *in vitro* because β-catenin is phosphorylated by JNK, which compromises its interaction with cadherins and consequently their tethering to the cytoskeleton (Lee et al., 2009, 2011; Naydenov et al., 2009). Hence ectopic JNK activity in cells lacking Cindr could account for changes in adhesion that release cells from the epithelium, as described below. However, JNK activity also commonly triggers apoptosis (Davis, 2000; Lin, 2003; Liu and Lin, 2005) and we found that JNK mediated the death of *cindr*-depleted cells. Hence Cindr-JNK interactions are necessary to regulate adhesion and the cytoskeleton to maintain cells within the epithelium and spare them from death. Indeed we found that *Drosophila* JNK (named Basket, Bsk) resides in complexes with Cindr that we argue are essential to curtail JNK activity.

2. Materials and methods

2.1. Drosophila genetics

All fly crosses were raised at 25 °C unless otherwise noted. We generated the fly lines *UAS-GMA*, *UAS-Dcr-2*; *ptc-GAL4*, *UAS-GFP* (X, II) and *ptc-GAL4*, *UAS-GFP*; *UAS-GMA* (*II*, *III*) with transgenic stocks obtained from the Bloomington Stock Center (BL-6874, BL-2017, BL-24646, BL-31774, BL-31776). We nicknamed these stocks GDPG and PGG respectively. The transgenic lines used to reduce Cindr are described in Johnson et al. (2008). *UAS-cindr*$^{RNAi2.21+23}$ combines two identical *RNAi* transgenes that target nucleotides 1016 to 1518 (nucleotide positions relate to the longest, predominantly expressed *cindr* transcript). A second line, *UAS-cindr*$^{RNA3.73+81}$ combines two identical *RNAi* transgenes that target nucleotides 1664 to 2246. Both *UAS-cindr*$^{RNAi2.21+23}$ and *UAS-cindr*$^{RNA3.73+81}$ reduce expression of long and intermediate Cindr isoforms (described in Johnson et al., 2008), but *UAS-cindr*$^{RNAi2.21+23}$ is three times more effective than *UAS-cindr*$^{RNA3.73+81}$ in reducing *cindr* transcripts. We therefore used *cindr*$^{RNAi2.21+23}$, abbreviated throughout the manuscript to *UAS-cindr*^{RNAi2}, for most studies. To assay the effects of reducing *cindr*, we crossed GDPG females to *UAS-cindr*^{RNAi2} males and dissected male third larval instar progeny, which had higher levels of *Dcr-2* expression than females. Stable stocks carrying *UAS-cindr*^{RNAi2} and *UAS-p35* (BL-5072) were generated and crossed to GDPG to block cell death in the *ptc*-domain of the progeny. Stable stocks carrying *UAS-cindr*^{RNAi2} and *UAS-bsk*^{DN} (BL-9311) or *bsk*^{1} (BL-3088) or *Jra*^{3} (Fanto et al., 2000, gift from Ursula Weber) were established and crossed to GDPG to assess whether reducing JNK signaling activity modified *cindr*^{RNAi2}-phenotypes. Again, only male larval progeny were dissected. *UAS-slpr*$^{WT\text{-}HA\text{-}55}$ (Garlena et al., 2010, gift from Beth Stronach) was combined with *UAS-cindrPC*^{TAP} (Johnson et al., 2008) to generate stable fly lines and crossed to PGG to test whether ectopic Cindr could quash ectopic JNK activity. When PGG was used as the maternal parent, both male and female larval progeny were dissected.

To assay JNK activity we generated stable fly lines that carried *ptc-GAL4, UAS-GFP* and *puc*^{E69} (*puc-lacZ*, BL-6762), *hid-lacZ* (Fan et al., 2010, gift from Andreas Bergman) or *TRE-RFP-16* (Chatterjee and Bohmann, 2012, gift of Dirk Bohmann) and crossed these to *UAS-cindr*^{RNAi2} males. For better detection of *TRE-RFP-16* expression, crosses were raised 29 °C. The *ptc-GAL4, UAS-GFP*; *puc*^{E69} line was also used to test whether *UAS-cindrPC*^{TAP} suppressed *UAS-slpr*$^{WT\text{-}HA\text{-}55}$-induced JNK activity.

High expression of *cindr*^{RNAi2} was mainly pupal-lethal. To generate pupal *cindr*^{RNAi2} tissue for live cell imaging, we maintained cultures of *UAS-cindr*^{RNAi2} crossed to GDPG at 18 °C until the progeny pupated. Male pupae were gathered at 0 h after puparium formation (APF), maintained at 25 °C, and imaged 14 h later. Live imaging is described below.

2.2. Dissection, immunofluorescence and microscopy

Wandering third instar larvae were dissected in PBS and fixed in 4% formaldehyde using standard procedures. Progeny of crosses utilizing GDPG or PGG were imaged within 24 h of dissection. For immunofluorescence, primary antibodies were rabbit anti-Cindr (1:300, Johnson et al., 2008), rat anti-*Drosophila* Ecadherin (1:50, DSHB DCAD2), rabbit anti-cleaved caspase-3 (Cell Signaling Technology, #9661S), mouse anti-MMP1 (1:10, DSHB 3B8D12-S), mouse-anti-Profilin (1:1, DSHB chi 1J), and rat anti-Twist (1:500, Roth et al., 1989, gift from E. Wieschaus). To visualize actin, Rhodamine Phalloidin was included in both fixative and primary antibody incubations (1:100–1:200, Molecular Probes R415). Secondary antibodies were conjugated to Alexafluor 488, Alexafluor 647 or Cy3 (Jackson ImmunoResearch). Cell death was determined using an In Situ Cell Death Detection Kit (TMR Red, Roche). Tissue was imaged with a Zeiss LSM 501 metaconfocal and Zen software.

To detect *puc-lacZ* or *hid-lacZ* expression, dissected wing discs were fixed in 2% gluteraldehyde and β-Gal activity detected using standard methods. Wing discs were imaged using a Zeiss Axioplan light microscope, Tucsen H series camera and ISCapture V3.0 software.

Adult wings were preserved in 100% Ethanol and then mounted in Euparal. These were imaged with a Zeiss Axioplan light

microscope described above.

The culture of pupae for live imaging is described above. Our live-imaging protocol was inspired by (Classen et al., 2008). At 14 h APF the pupal case was partially removed to reveal one wing and the pupa arranged on a microscope slide to display the exposed wing and stabilized with double-sided tape. Oxygen-permeable hydrocarbon oil was placed directly on to the pupa to cover the wing and prevent dehydration before cover-slipping. This preparation was then directly imaged with confocal microscopy.

All images were prepared for publication using Adobe Photoshop. Minimal adjustments were applied to the whole image and equal minimal adjustments applied to images of control and experimental tissue. Maximal Image Projection of confocal serial sections were generated using ZEN2009 software.

2.3. Phenotypic analyses and statistics

To determine *puc-lacZ* or *hid-lacZ* expression in larval wing discs, the relative pixel intensities were determined using NIH Imager as follows: the pixel intensity of a rectangle approximately spanning the *ptc*-domain at the dorsal-ventral boundary was determined and the pixel intensity of a neighboring equal-sized control sample (within the posterior domain of the wing disc) subtracted. The Students' *T*-test was used to determine statistically relevant differences in pixel intensity (β-Gal activity).

Adult wings were analyzed with NIH ImageJ to determine the relative area between the L3 and L4 longitudinal wing veins. For each wing, this area was normalized by division by the area of the entire wing blade. Students' *T*-tests and one-way ANOVAs were used to determine statistically relevant differences in the size of this domain.

To determine differences in mean apical area of cells anterior to the *ptc* expression domain, within the *ptc* domain and immediately posterior to the A/P adherens boundary in *ptc > Dcr-2, GFP, cindr*^{RNAi2} and *ptc > Dcr-2, GFP, lacZ* wing discs, 96 cells were randomly selected in each of these three zones from 4 different wing discs. Areas were calculated using NIH ImageJ. Students *T*-tests were used to determine statistically relevant differences in apical cell area.

To score the modification of *ptc > Dcr-2, cindr*^{RNAi2} by partially disabling JNK signaling, the phenotypes of wings were ranked independently, three times. When assessing rescue of the *ptc* domain integrity, the width of the *ptc* domain was compared to wild type control and *cindr*^{RNAi2}-expressing wings. Wings were scored as no modification (same width as *ptc > Dcr-2, cindr*^{RNAi2}), mild rescue (10–30% improvement in the width of the domain), moderate rescue (50–75% improvement in *ptc*-domain width) and strong rescue (100–75% the width of the *ptc* domain of *ptc > Dcr-2, cindr*^{RNAi2} wings). To assess modifications in the migratory behavior of cells, the amount cell displacement posterior to the A/P adherens boundary was assessed and wings scored as no modification (0–10% change in cell displacement), weak rescue (10–30% reduction in cell displacement), moderate rescue (30–80% reduction) and strong rescue (80–100% reduction in cell displacement). Statistical analyses were not performed on these analyses as the number of discs assessed (between 14 and 21 of each genotype) was deemed too low.

2.4. Co-immunoprecipitation analyses

Cindr-dJNK complexes were co-immunoprecipitated from *CantonS* embryos or embryos in which *UAS-bsk*^{myc} (Rallis et al., 2010, gift from Julian Ng) or *UAS-cindrPC* (Johnson et al., 2008) were driven with the *dauthterless-GAL4* driver line (BL-5460) using standard protocols. For this we utilized rabbit anti-Cindr (Johnson et al., 2008), rabbit anti-JNK (Santa Cruz Biotechnology, sc-571) or rabbit anti-JNK (Cell Signaling Technology, #9252), rabbit anti-pJNK (Promega Corporation, V793) or mouse anti-pJNK (Cell Signaling Technology #9255) and mouse anti-myc (Cell Signaling Technology, 9B11). Samples were analyzed using standard Western Blot analysis.

3. Results

3.1. Loss of Cindr compromised epithelial integrity

Reducing Cindr in the developing *Drosophila* wing revealed an important role for Cindr in the correct development and integrity of this epithelium. Specifically, we used the *patched-GAL4* driver line (*ptc-GAL4*) to express short hairpin RNA interference (RNAi) transgenes that targeted *cindr* (*UAS-cindr*$^{RNAi.21+23}$) (Johnson et al., 2008) in a central panel of the developing wing – the *ptc* expression domain (Fig. 1A). We abbreviate the genotype of these animals to *ptc > cindr*^{RNAi2} throughout this manuscript. For wild-type control wing tissue we expressed *green fluorescent protein* (GFP) or β-*Galactosidase* (β-*Gal*) (*ptc > GFP* and *ptc > lacZ* respectively). Reducing Cindr led to almost complete absence of the *ptc* domain from the adult wing (Fig. 1B–D), suggesting that reducing *cindr* in this tissue during wing development led to loss of the majority of these cells.

This mass reduction in tissue has not been reported in other *Drosophila* tissues requiring Cindr. For example, reducing Cindr in the pupal fly eye does not reduce final eye size. Instead Cindr is required for correct local cell movements that organize cells into stereotypical positions (Johnson et al., 2008, 2011, 2012). This function is mediated through interactions with actin regulatory proteins that bind Cindr, including the CPs that limit and stabilize actin polymerization and GAPs that inactivate Arf6 (Johnson et al., 2008, 2011). These interactions underscore a requirement for Cindr to keep actin polymerization in check during eye morphogenesis. In addition Cindr regulates adhesive junctions to promote maintenance of correctly arranged cells during eye patterning (Johnson et al., 2008, 2012). Given these observations, we wondered whether reducing *cindr* in the *ptc*-domain of the wing modified actin and adhesion to promote cell behaviors that compromised wing cell viability. We addressed this question by examining the behavior of *cindr*^{RNAi}-expressing cells in larval and pupal wing epithelia.

Reducing *cindr* using two independent RNAi transgenes disrupted the larval and pupal wing epithelia (Figs. 2, 3 and S1). *UAS-cindr*$^{RNAi.21+23}$ (abbreviated to *cindr*^{RNAi2}) more effectively reduces *cindr* than *UAS-cindr*$^{RNA3.73+81}$ (*cindr*^{RNAi3}) (Johnson et al., 2008, 2012) and was therefore used for all further investigations. To enhance detection of the cell body, filopodia and apical zonula adherens (ZA) we expressed cytoplasmic and nuclear *GFP* as well as *GMA* (a GFP:moesin-actin-binding-domain fusion protein that interacts with actin filaments) in *ptc*-domain cells. Reduction of Cindr in the larval wing disc triggered mass displacement of cells from the *ptc*-domain (compare Fig. 2B–C with D–E). The *ptc*-domain abuts the anterior–posterior (A/P) boundary (Fig. 2A and B). In *ptc > cindr*^{RNAi2} wings we identified an A/P 'adherens boundary' which we define here as that most-posterior column of cells with clearly defined ZAs marked by GMA accumulation (Fig. 2D and D′). The A/P adherens boundary likely coincides with the A/P compartment boundary defined by lineage analysis, gene expression and Myosin II-dependent cell bond tension (Garcia-Bellido et al., 1973; Lawrence and Struhl, 1996; Landsberg et al., 2009), unless these features are disrupted by expression of *cindr*^{RNAi2} (not tested). Many *cindr*^{RNAi2}-cells were observed posterior to the A/P adherens boundary (Fig. 2D′) and the width of the 'intact' *ptc*-

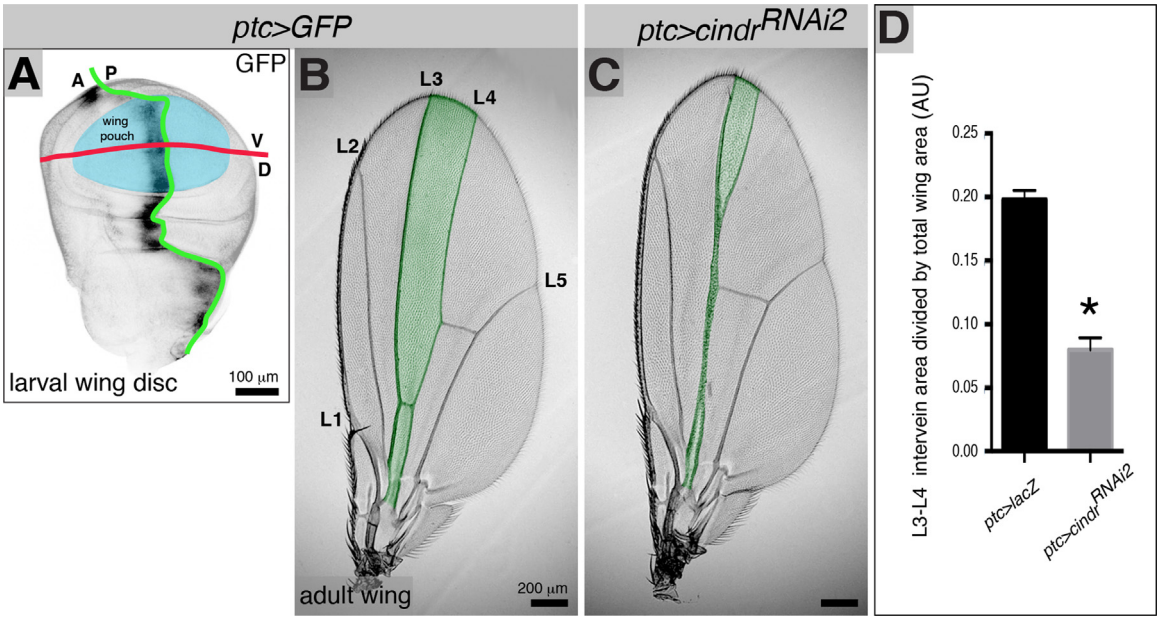

Fig. 1. Reducing Cindr in the *ptc*-expression domain disrupted wing patterning. (A) Wing disc dissected from a third instar larva expressing *GFP* in the *ptc* expression domain (GFP shown in black). *GFP* expression extends anteriorly from the boundary between anterior (A) and posterior (P) compartments, traced by a green line. A red line traces the dorsal-ventral boundary of the wing, which bisects the wing pouch that will give rise to the adult wing blade, colored blue. (B–C) Representative *ptc > lacZ* and *ptc > cindr^{RNAi2}* adult wings. Green pseudocolor highlights the region between the L3 and L4 wing veins that approximately corresponds to the *ptc*-expression domain. These wings are oriented with anterior to the left. Longitudinal veins are labeled L1-5. (D) Quantification of relative areas of the *ptc*-domain indicated significant loss of tissue (*, $p < 0.0001$) from *ptc > cindr^{RNAi2}* adult wings when compared to control *ptc > lacZ* wings. The area between L3 and L4 veins was taken as a proxy for the *ptc* domain. This area was normalized by division by the area of the entire wing blade. This region constitutes approximately 20% of the wing area in control animals but only 8% in *ptc > cindr^{RNAi2}* wings. Twenty-five wings of each genotype were analyzed. Error bars represent standard deviation.

domain – taken as those columns of cells anterior to the A/P adherens boundary – was dramatically reduced (Fig. 2B′ and D′). The larval wing disc is a pseudostratified monolayer epithelium. Most displaced *cindr^{RNAi2}*-cells lay within the lower half of the epithelium, having lost contact with the apical epithelial surface (compare Fig. 2C and E and Fig. 3B to E). Expression of *cindr^{RNAi3}* less effectively reduced *cindr* transcripts (Johnson et al., 2008) but also induced delamination of cells (Fig. S1E–F).

To understand the morphology of displaced *cindr^{RNAi2}*-cells better, we examined the effect of reducing Cindr in cuboidal epithelial cells of the pupal wing. At 14 h after puparium formation (h APF), these cells are four to five times larger than cells of the larval wing epithelium. At 14 h APF the wing is rather like an oval water balloon: the single-layered cuboidal epithelium encloses a fluid-filled lumen. We peeled back the chitinous pupal-case to expose the dorsal surface of the wing for live-imaging (Fig. 2F). Using this strategy we observed GFP-labeled cells projecting dynamic extensions and confirmed that in *ptc > GFP* wings, cells remained in stable positions, shifted only by occasional cell division (Fig. 2G, data not shown). In contrast, reducing Cindr released small groups and individual cells from the epithelium (Fig. 2H–K). These cells delaminated into the underlying lumen and we expect were later swept away in the fluid hemolymph. Whilst delaminating, some cells adopted morphologies reminiscent of migrating mesenchymal cells (Fig. 2I). These observations support the hypothesis that in the absence of Cindr, epithelial cells delaminate and acquire migratory potential.

3.2. Features associated with cell delamination and migration accompanied loss of Cindr

The apical circumferences of many *cindr^{RNAi2}*-cells still within the ‘intact’ *ptc*-domain (defined above) were mildly reduced (compare Fig. 3F′ and G′, H-b and I-b, quantified in Fig. S3), indicating apical constriction which often portents cell delamination (Katoh and Fujita, 2012; Eisenhoffer and Rosenblatt, 2013). Consistent with this suggestion, we observed several small *cindr^{RNAi2}*-cells distributed through the *ptc* domain (examples are colored green in Fig. 3I-c) as well as groups of cells arranged in rosettes (examples are colored pink in Fig. 3I-c) – we expect that a cell originally lay in the center of these rosettes, but had delaminated. These observations are consistent with those of delamination in other systems (for eg. Marinari et al. (2012) and Muliyil et al. 2011)) and described by T2 transition models (Fletcher et al., 2014). Interestingly, the apical circumferences of several rows of cells posterior to the A/P adherens boundary were enlarged (Fig. 3I-b, for quantification see Fig. S3) – the cause of this non-autonomous effect of reducing Cindr requires further investigation.

In each wing disc between one and five plump round *cindr^{RNAi2}* -cells were observed still within the apical third of the epithelium, but well away from the *ptc*-domain (for example, Fig. 3C and D). We also frequently observed large cells at or near the A/P adherens boundary that were oval in shape (for eg. cell marked with arrow in Fig. 3I-d). These were located within the apical third of the epithelium and appeared to protrude into the posterior region across the A/P adherens boundary (Fig. 3I-a, compare to Fig. 3H-a). Enriched F-actin in most of these larger apical cells suggested reorganization of the actin cytoskeleton (Fig. 3I-d and I-e, compare to Fig. 3H-d and H-e). We conclude that in addition to basal delamination, some *cindr^{RNAi2}*-cells were released apically into the posterior compartment. This would require crossing or eroding a Myosin cable that spans the length of the wing to separate anterior and posterior compartments (Landsberg et al., 2009). How this occurs is the subject of future investigation.

Ecadherin is not only detected at AJs but also along the length of the lateral membranes of wing epithelial cells, albeit at lower concentrations – Ecadherin outlines the basal circumference of these cells (Fig. 3J′). Reducing Cindr disrupted cell morphology so extensively that the honey-comb pattern of basal Ecadherin was

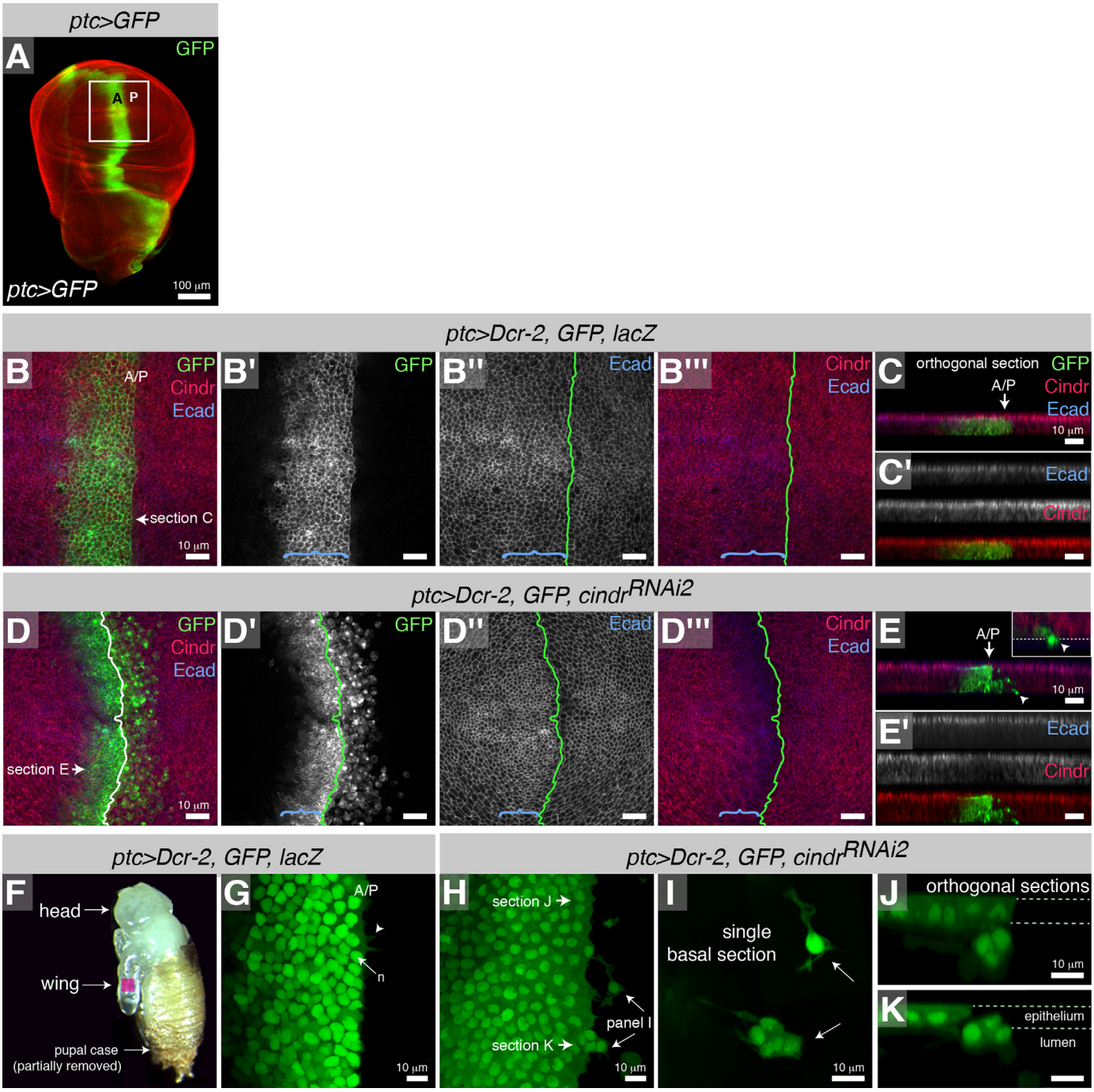

Fig. 2. Reducing Cindr in the *ptc*-expression compromised epithelial integrity. (A) Whole wing disc dissected from a third instar larva expressing *GFP* in the *ptc* expression domain, which abuts the A/P adherens boundary. The white box represents the region of the larval wing pouch presented in panels B, D and throughout this manuscript. (B–C) In the wing pouch of control *ptc > Dcr-2, GFP, lacZ* larval wing discs, GFP is localized through the nucleus and cytoplasm and accumulates at the ZA (B′), also marked by Ecadherin localization (B′′). GFP expression ends abruptly at the A/P adherens boundary. Blue brackets mark approximate width of the *ptc* domain. A green line marks the A/P adherens boundary in B′′ and B′′′. Cindr is ubiquitously expressed (red, B′′′) and apically enriched at AJs (Ecadherin, C and C′). The position of this orthogonal section is indicated on panel B (arrow). (D–E) Many cells expressing *cindr*^{RNAi2} as well as *Dcr-2* and *GFP* are displaced across the A/P adherens boundary into the posterior compartment. The A/P adherens boundary is marked by a white line in D, green line in D′–D′′′, and arrow in E. The approximate width of the 'intact' *ptc* domain (anterior to the A/P adherens boundary) is indicated with a blue bracket (D′). Most cells that cross the A/P adherens boundary (D′) have delaminated from the epithelium. Displaced cells are quickly replaced to maintain a confluent epithelium (D′′). Cindr is efficiently reduced in a graded manner across the *ptc* domain (D′′). Delaminated and displaced *cindr*^{RNAi2}-cells are clearly observed in orthogonal sections (E and E′, position indicated on D). Inset provides a higher magnification image of a cell emerging basally from the epithelium (arrow-head; dotted line indicates base of the epithelium). (F) The pupal case is partially removed for imaging of small regions of the dorsal pupal wing epithelium. Pink box represents region imaged. (G) Expression of GFP in the *ptc* domain enabled live imaging of the larger cuboidal cells of the pupal wing. GFP is enriched in cell nuclei (n) and some cells project filopodia across the A/P adherens boundary (arrowhead).(H–K) Live-imaging of *ptc > Dcr-2, GFP,cindr*^{RNAi2} wings captured single and groups of cells emerging from and basal to the epithelium (H, I). Delaminated cells entered the underlying haemolymph-filled lumen. Migratory cell morphologies were occasionally observed (I). Basally delaminating cells are easily observed in orthogonal sections (J–K).

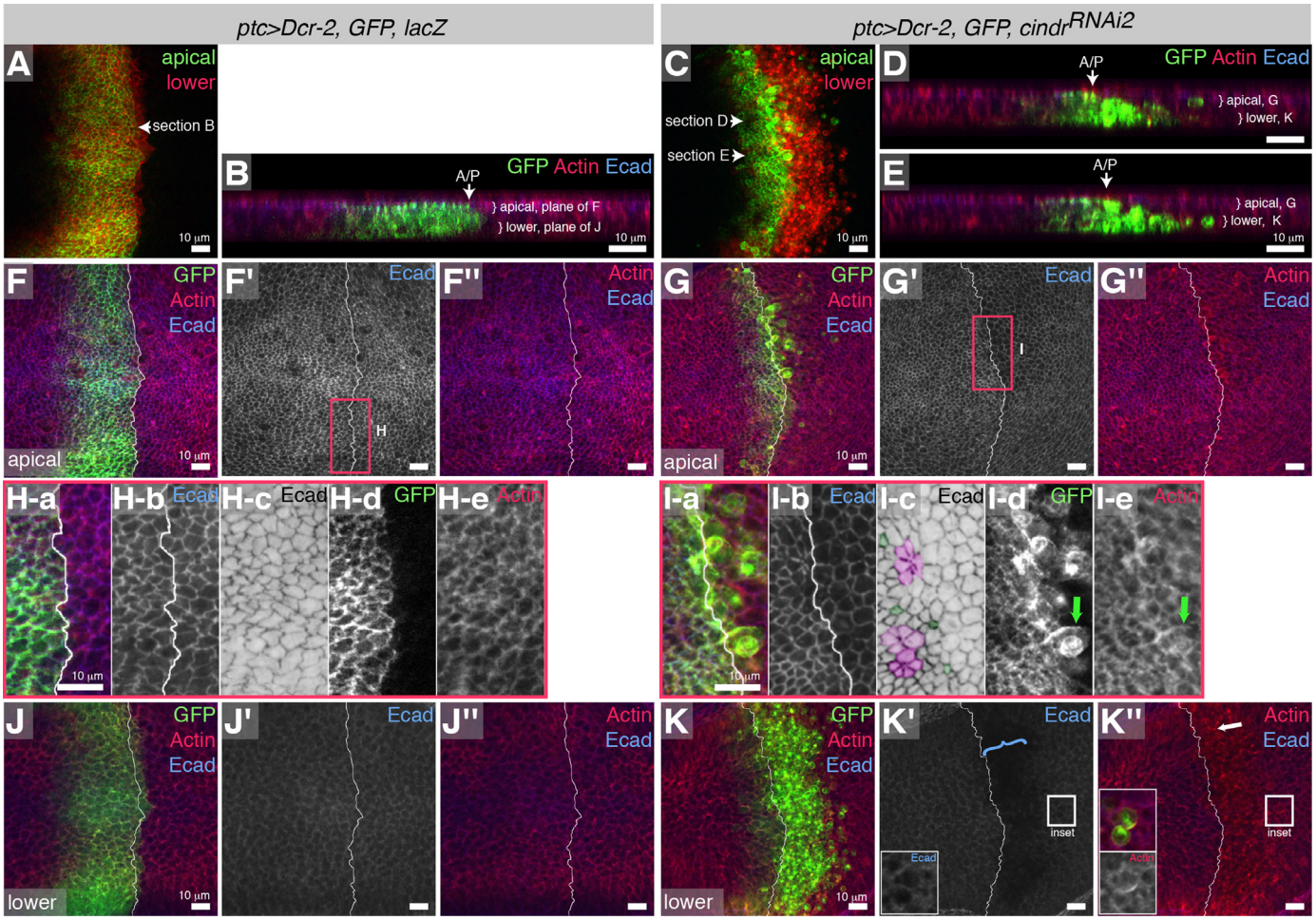

Fig. 3. Reducing Cindr triggered basal delamination and lateral cell movement. (A–B) Overlays of the apical 1.23 μm (green), and lower 1.23 μm zones (red) of a *ptc > Dcr-2, GFP, lacZ* larval wing pouch. Apical and lower zones are indicated in B; please refer to Fig. S4 for helpful illustration of the wing. In an orthogonal cross section of this wing (B) we observe some 'bulging' of GFP-cells beneath the surface of the A/P adherens boundary (indicated). (C–E) The apical 1.23 μm (green), and lower 1.23 μm zones (red) of a *ptc > Dcr-2, GFP, cindr^{RNAi2}* wing. In two orthogonal cross sections (D,E) we observe substantial movement of cells across the A/P adherens boundary. Position of these cross-sections indicated in C. (F–G) The apical zones (only) of control *lacZ* and *cindr^{RNAi2}*-expressing tissue. Actin (red) and Ecadherin (blue, white in F′ and G′) are also shown. Red boxes indicate tissue presented at higher magnification in H and I. A/P boundaries are indicated with white lines. (H–I) Higher magnification images of a small region of tissue straddling the A/P adherens boundary (marked by white lines). In control tissue, GMA (GFP), Actin and Ecad accumulate apically marking the ZA. Higher levels of Ecadherin are detected at the smaller circumferences of *cindr^{RNAi2}*-cells. Cells arrange into rosettes (pink) and numerous diminutive cells (green) are also observed. Green arrows indicates a large oval cell migrating apically, enriched in actin. (J–K) The lower 1.23 μm zones of *lacZ* and *cindr^{RNAi2}*-expressing tissue. Actin (red) and Ecadherin (blue, white in J′ and G′) are homogenously localized about the periphery of cells in control wings (J′), marking the lateral membranes. A marked decrease in Ecadherin and increase in Actin is observed in most basal *cindr^{RNAi2}*-cells (blue bracket, K′, white arrow (K″) indicates an F-actin punctum), except in several 'healthier' migrating cells that retain peripheral Ecadherin (inset in K′–K″).

destroyed (Fig. 3K′). In fact, little Ecadherin was detected in most of the mass of basal *cindr^{RNAi2}*-cells but in contrast, actin was enriched (Fig. 3K″, compare to Fig. 3J″). As discussed below, many of these cells died. Consequent collapse of the actin cytoskeleton may have accounted for the bright phalloidin and GMA puncta observed (white arrow in Fig. 3K″). However, in several large round *cindr^{RNAi2}*-cells located in the posterior compartment we detected a modest increase in peripheral F-actin (Fig. 3K″, inset). Peripheral Ecadherin was also observed in these cells (Fig. 3K′, inset). We hypothesize that increased F-actin powered migration of these cells and peripheral Ecadherin mediated their transient attachment to neighboring cells. A similar mechanism drives collective migration of the border cells within the *Drosophila* ovary (Cai et al., 2014; Niewiadomska et al., 1999; Fulga and Rorth, 2002). Consistent with active remodeling of the cytoskeleton, Profilin (Chickadee in *Drosophila*, Chic) was enhanced within *cindr^{RNAi2}*-cells (Fig. S4A–B) and an antibody to matrixmetalloprotease 1 (MMP1) provided a snapshot of increased MMP production and release that would degrade extracellular matrix proteins and make way for migratory cells (Fig. S4C–D). These features often accompany transformation of epithelial cells to mesenchymal fates (Lim and Thiery, 2012; Parisi and Vidal, 2011; Baum et al., 2008), but we detected only occasional expression of the mesenchymal marker Twist in migrating *cindr^{RNAi2}* -cells (Fig. S5A–B and data not shown). Taken together, these data suggest that reducing Cindr enables delaminating cells to actively migrate from the *ptc* expression domain. However, cells could also be passively dispersed into the posterior compartment after delamination.

3.3. *Most cindr^{RNAi2}-cells that escaped the ptc-domain died*

The majority of delaminated *cindr^{RNAi2}*-expressing cells were small or fragmented, consistent with cell collapse and fragmentation during apoptosis or anoikis. Terminal deoxynucleotidyl transferase (TdT)-mediated dUTP nick end labeling (TUNEL) confirmed wide-scale cell death (Fig. 4B, compare to Fig. 4A). We also detected significant activation of Caspase-3 (Fig. 4D, compare to 4C) and Dcp-1 (data not shown), caspases that mediate apoptosis.

The vast majority of delaminating larval wing cells died within

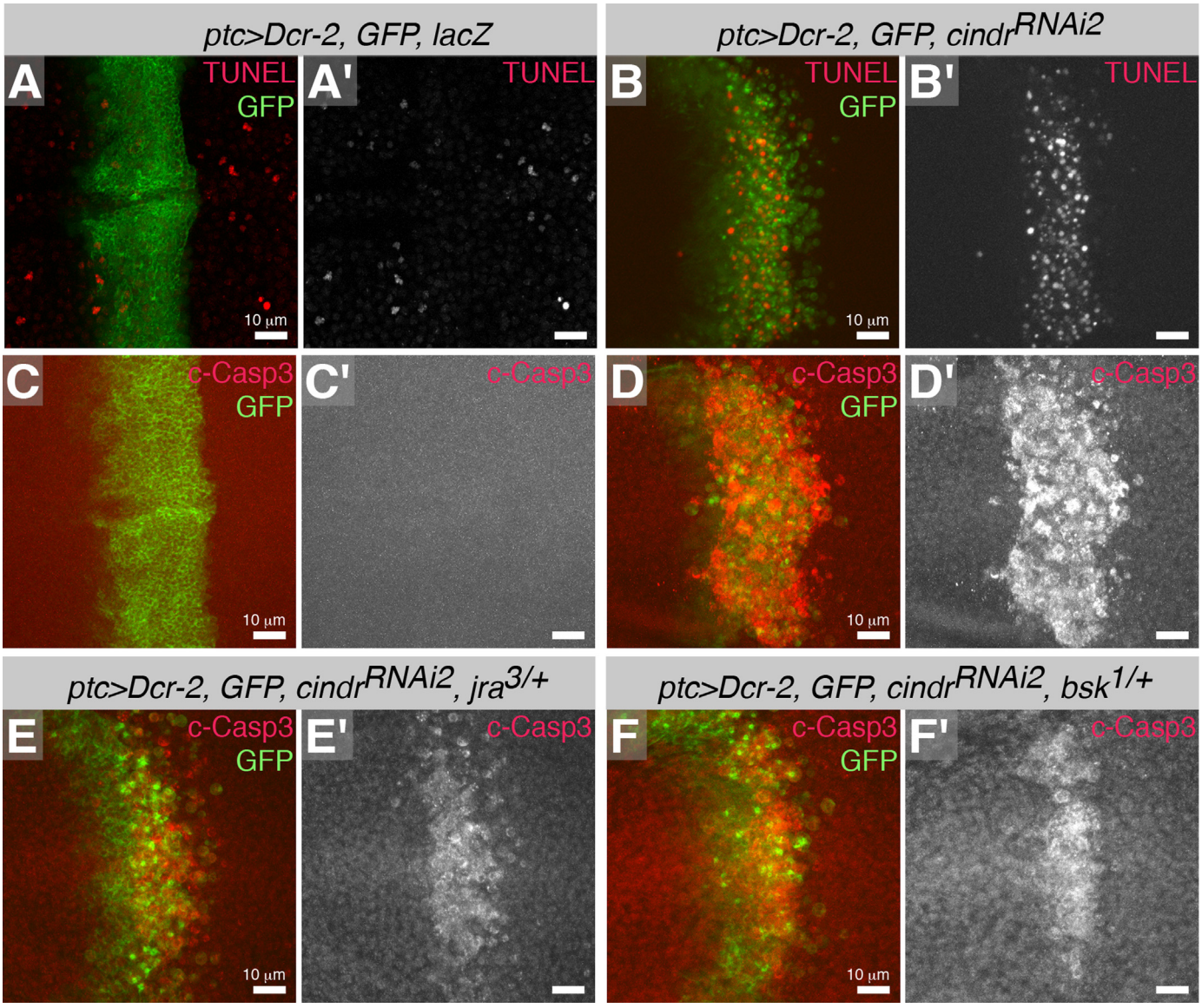

Fig. 4. Reducing Cindr triggered cell death. (A–B) Extensive TUNEL (red) was detected in *ptc > Dcr-2, GFP, cindr*^{RNAi2} wing discs (B) but not *ptc > Dcr-2, GFP, lacZ* tissue (A). (C–D) Activated cleaved caspase-3 (red) was detected in *cindr*^{RNAi2}-cells as well as numerous neighboring non-*GFP*, non-*cindr*^{RNAi2} cells (lack of overlay between green and red channels, D). (E–F) In tissue heterozygous for the transcription factor dJun (*jra*, E) or dJNK (*bsk*, F), reduced activated cleaved caspase-3 (red) was detected in *cindr*^{RNAi2}-cells, indicating reduced cell death.

a short distance from the intact *ptc*-domain. This raised the concern that large round or oblong cells described above as migrating were rather simply displaced by the mass of basal dying cells. We also questioned whether delamination was triggered by cell death or was an active process independent of cell death. To address these questions we co-expressed *p35* in *cindr*^{RNAi2}-cells to repress apoptosis (Hay et al., 1994). This strategy generated a broad, twisting panel of *cindr*^{RNAi2}-cells (Fig. S5B and D, compare to S5A). Numerous individual cells were still observed migrating from the *ptc*-domain (Figs. S5B and D). These data confirmed that apoptosis was not essential for the release of *cindr*^{RNAi2}-cells from the epithelium. However we cannot discount that at least some *cindr*^{RNAi2}-cells are passively dispersed consequent to severe morphological disruption of these wing discs.

The behaviors of *cindr*^{RNAi2}-cells were remarkably similar to those described as oncogenic-like cell invasion in several models that similarly utilized the *Drosophila* larval wing. In these models the activity of Csk, Src, Rho1, Abl, Ret, Ras, Cpa or Sin3a were modified (Vidal et al., 2006; Singh et al., 2010; Vidal et al., 2010; Das et al., 2012; Rudrapatna et al., 2013; Dar et al., 2012; Cordero et al., 2010; Fernandez et al., 2014; Speck et al., 2003; Neisch et al., 2010). In each case, JNK signaling mediated cell migration and death. To test whether JNK was employed to trigger the death of *cindr*^{RNAi2}-cells, we partially impeded JNK activity by reducing *Drosophila* JNK (encoded by *bsk* but referred to hereafter as dJNK) or Jun (Jra or dJun) function. JNK is the final kinase in a cascade that activates transcription factors including Jun. Reducing dJNK or dJun reduced Caspase-3 activation in *cindr*^{RNAi2}-cells (Fig. 4E and F, compare to 4D). This implied that JNK activity contributed to the death of delaminated *cindr*^{RNAi2}-cells. Below we describe other behaviors of *cindr*^{RNAi2}-cells mediated by JNK.

3.4. Cindr and dJNK (bsk) reside in complexes

Notably, Cindr and dJNK were identified as interactors in two independent proteome-wide yeast two-hybrid (Y2H) screens that utilized either Gal4- or LexA-based Y2H strategies (Giot et al., 2003; Stanyon et al., 2004). These findings suggested that a direct

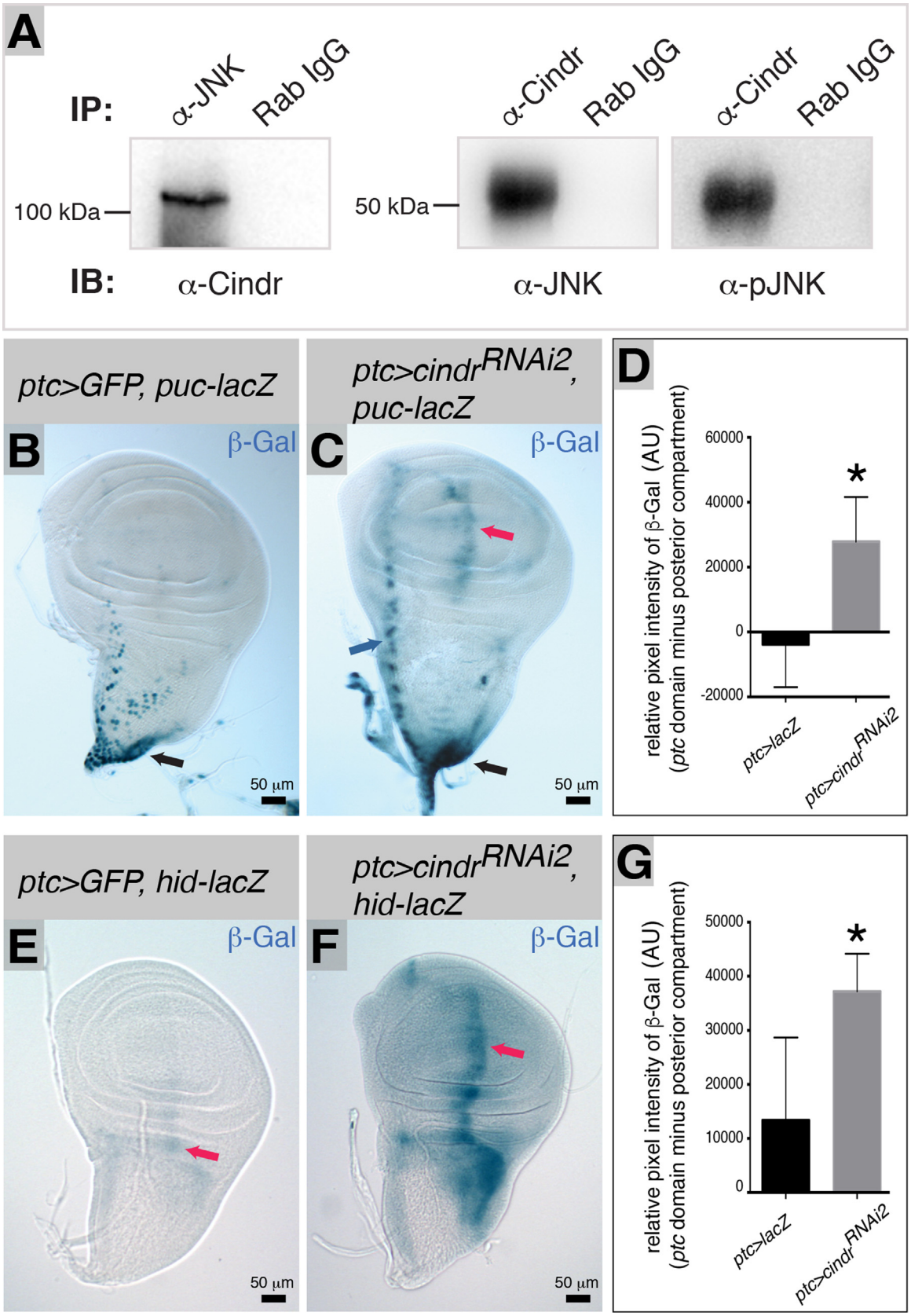

Fig. 5. Cindr and dJNK were identified in endogenous complexes and regulated JNK signaling activity. (A) Co-immunoprecipitations of dJNK (left panel) and Cindr (right hand panels) from wild type Canton S embryos confirmed that both proteins resided in a protein complex. Blots were probed with antibodies to Cindr (left), JNK (middle) and phosphorylated JNK (right). (B–C) Mild reduction of *cindr* (C) in the *ptc*-domain activated the *puc-lacZ* transcriptional reporter (red arrow), a target of Jun/Fos transcription factors that are activated by dJNK. Little *puc-lacZ* expression was detected in the wing pouch of control wing discs (B). Endogenous JNK activity drives *puc-lacZ* expression in the dorsal region of the wing disc (black arrows) and a strip of cells in the overlying peripodial membrane (blue arrow). (D) Quantification of *puc-lacZ* expression (detection of β-Gal activity). Significantly more enzymatic activity was detected in *ptc > cindr*^{RNAi2} wing pouches ($p < 0.00001$, $n = 21$) in comparison to *ptc > GFP* wing pouches ($n = 20$). To correct for background enzymatic activity, pixel intensity of a sample in just posterior to the A/P adherens boundary was subtracted from an equivalently-sized neighboring sample in the *ptc*-domain. Tissue posterior to the A/P adherens boundary of many *ptc > GFP* wings had a mildly higher pixel intensity tissue within the *ptc*-domain resulting in a negative relative intensity for this genotype. AU, arbitrary units. (E–F) Reduction of *cindr* (F) activated *hid-lacZ* transcription (red arrow). Some background *hid-lacZ* expression was detected in control *ptc > GFP* wings (**F,** red arrow). (G) Quantification of *hid-lacZ* expression. Significantly more enzymatic activity was detected in *ptc > cindr*^{RNAi2} ($p < 0.00001$, $n = 27$) than *ptc > GFP* ($n = 16$) wing pouches. Error bars represent standard deviation. AU, arbitrary units.

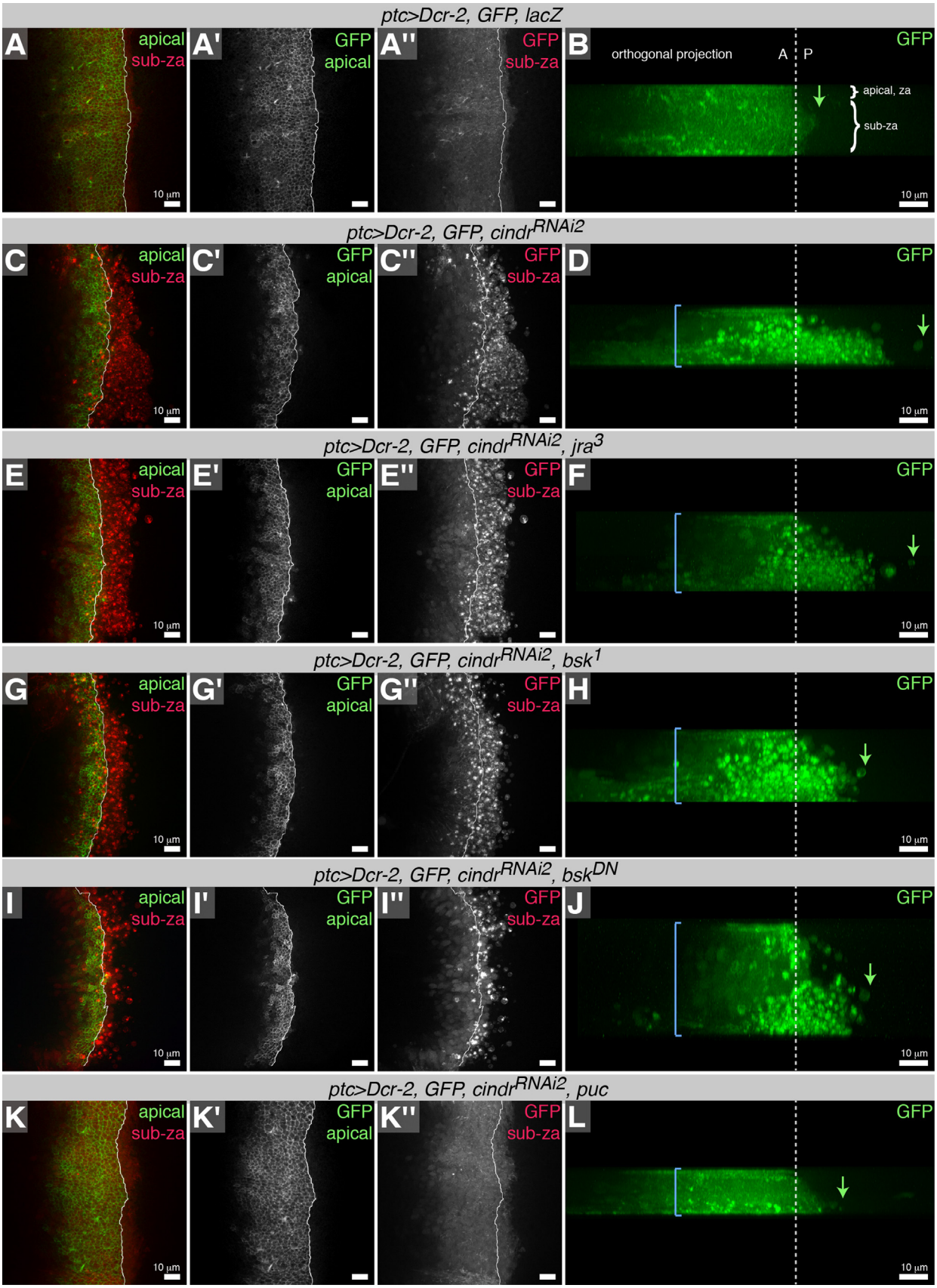

Fig. 6. JNK signaling mediated the migratory behavior of *cindr*^{RNAi2}-expressing cells. In all left-hand panels, maximum projections of confocal sections that encompassed the ZAs (green, referred to as apical) are overlaid onto maximum projections of all confocal sections gathered below the ZA zone (red, sub-ZA). Orthogonal projections (right-hand panels) are of the same wings presented *en face*. (A–B) Expression of *lacZ* in the *ptc*-domain disturbed neither cell nor tissue morphology. The A/P adherens boundary is illustrated with a white line and apical and sub-ZA projections provided separately. In orthologonal projections of this same wing disc, we observe a minor 'bulge' in the GFP-labeled tissue (green arrow, B). A straight dotted white line marks the apical limit of the A/P adherens boundary in B. (C–D) Reducing *cindr* triggered cell movement. In orthogonal projections we observed a mass of delaminated and migrating cells (D). Green arrow marks a cell that migrated further into the posterior compartment. A blue bracket indicates the depth of the wing pouch. (E–J) Compromising JNK activity in *jra* (E–F) or *bsk* heterozygotes (G–H), or wings co-expressing *bsk*^{DN} (I–J) mildly reduced cell delamination and migration. Green arrows mark the cell furthest from the A/P adherens boundary in F, H, J. Depth of the tissue (blue brackets) was increased in comparison to the *ptc* > *cindr*^{RNAi2} disc. (K–L) Repressing JNK activity via *puc* expression in *cindr*^{RNAi2}-cells largely repressed cell delamination and migration. Occasional cells were observed beyond the A/P adherens boundary (green arrow in L).

link between JNK signaling and Cindr may have crucial functions in epithelia. We confirmed that Cindr and dJNK resided in complexes *in vivo* using multiple approaches. We co-immunoprecipitated endogenous Cindr and dJNK from wild type *Drosophila* embryos (Fig. 5A). Complexes of ectopically expressed Cindr and dJNK were also identified *in vivo* (Fig. S6 and data not shown). Further, we identified activated, phosphorylated dJNK (pJNK) amongst the Cindr co-immunoprecipitate (Fig. 5A). Hence at least some dJNK is activated when complexed with Cindr. This led us to question whether Cindr interacts with dJNK to modify the activity of JNK signaling.

3.5. Cindr regulates dJNK signaling

To address the role of Cindr-dJNK complexes *in vivo* we assayed the response of JNK signaling in cells in which Cindr was only mildly reduced. Our intention was to avoid extensive cell delamination and death observed when we severely reduced Cindr because such disruption could independently trigger stress or wound-healing responses that activate JNK. Thus reducing Cindr below the threshold required for mass cell delamination and migration enabled us to isolate the direct effects of perturbing Cindr-dJNK complexes. To achieve this, we drove $cindr^{RNAi2}$ in the absence of Dcr-2 (Figs. 5 and Fig. S7), an approach that modestly reduced Cindr (Johnson et al., 2008). In these wing discs we detected activity of three independent transcriptional reporters that are targets of JNK signaling: *puckered-lacZ* (*puc-lacZ*, Fig. 5B–D, Fig. S7A–B, (Adachi-Yamada, 2002)), *head involution defective-lacZ* (*hid-lacZ*, Fig. 5E–G, (Fan et al., 2010)) and *TRE-red* (Fig. S7C–E (Chatterjee and Bohmann, 2012)). In a fourth assay we examined accumulation of Chic, also a transcriptional target of JNK signaling (Jasper et al., 2001). Higher levels of Profilin (Chic) accumulated in many basal $cindr^{RNAi2}$-cells (Fig. S4A–B, note that *Dcr-2* was co-expressed in these wing discs). Because Profilin facilitates actin polymerization, increased Chic could be indicative of activation of the cytoskeleton to drive cell migration. In contrast, expression of *hid-lacZ* (also a proxy for expression of pro-apoptotic *hid*) suggested that the apoptotic machinery had been engaged. Taken together, these data confirmed that wild-type levels of Cindr are required to quash JNK signaling in the developing wing epithelium. We propose that when complexed with Cindr, activated dJNK is repressed.

3.6. JNK activity mediates $cindr^{RNAi2}$ phenotypes in wing epithelia

Earlier, we discussed that JNK activity mediated the death of $cindr^{RNAi2}$-cells (Fig. 4D–F). To confirm that JNK also mediated the movement of $cindr^{RNAi2}$-expressing cells, we employed several strategies to simultaneously dampen JNK activity (Fig. 6). First, we expressed $cindr^{RNAi2}$ in the *ptc*-domain of wings heterozygous for *dJNK* (*bsk*) or one of its transcription factor targets *dJun* (*jra*) (Fig. 6E–H). Second, we expressed a dominant negative *dJNK* isoform (bsk^{DN}) together with $cindr^{RNAi2}$-transgenes (Fig. 6I–J). We observed insignificant improvements to the integrity and width of the 'intact' *ptc*-domain in these wings, when compared to $ptc > cindr^{RNAi2}$ wings (compare Fig. 6C′ to E′, G′ and I′. These data are quantified in Fig. S8A). In contrast, cell migration was curbed (compare Fig. 6C′′ to 6E′′, G′′ and I′′, and Fig. 6D to F, H and J). Specifically, when JNK signaling was impeded, we observed a reduction in the number of $cindr^{RNAi2}$-cells that lay in the posterior compartment and the distance that cells moved beyond the A/P adherens boundary in 86%, 81% and 63% of wing discs heterozygous for *dJNK* ($n=14$), *dJun* ($n=15$) or expressing bsk^{DN} ($n=21$), respectively (Fig. S8B). These data suggest that modest reduction in JNK signaling did not affect delamination of $cindr^{RNAi2}$-cells, but rather reduced the ability of these cells to disperse. This modification of cell behavior, compounded with a decrease in cell death, likely accounted for an increase in the thickness of the epithelium (compare Fig. 6F, H and J to C), especially obvious in wings co-expressing bsk^{DN} with $cindr^{RNAi2}$ (Fig. 6J).

To more severely impede JNK activity, we co-expressed *puckered* (*puc*), which deactivates dJNK (Martin-Blanco et al., 1998), with $cindr^{RNAi2}$-transgenes. This strategy dramatically rescued the integrity of the *ptc*-domain in 100% of the wing discs dissected ($n=18$, compare Fig. 6K and L to C and D). Little cell delamination and movement were observed, suggesting that directly inactivating dJNK completely removed the requirement for Cindr in this tissue. In support of this hypothesis, expression of *puc* completely restored the tissue between the L3 and L4 veins of the adult wing, which was lost when *cindr* expression was reduced throughout wing development (compare Fig. 7C to B). Expression of *puc* in otherwise wild-type cells of the *ptc* domain had no effect on cell morphology or behavior (data not shown) or the relative size of the L3–L4 intervein area (Fig. 7D).

3.7. A balance of Cindr and JNK activity maintained epithelial integrity

When taken together, our data suggests that activated dJNK is repressed when complexed with Cindr. This mechanism could limit JNK signaling in tissues rich in Cindr, including the wing (Fig. 2B), unless concentrations of activated dJNK outpaced that of Cindr. To test this hypothesis, we elevated the expression of the dJNK kinase kinase *slipper* (*slpr*) in the *ptc* domain (Stronach and Perrimon, 2002). This effectively triggered JNK-signaling (assessed by *puc-lacZ* expression, Fig. 8B compare to A). The uneven spread of *puc-lacZ* expression in these wing discs correlated with movement of cells beyond the A/P adherens boundary (Fig. 8G, compare to F) in 81% of $ptc > slpr$, *GFP*, *puc-lacZ* wing discs ($n=16$), which phenocopied cell displacement in $ptc > cindr^{RNAi2}$ wing discs. Next we introduced ectopic Cindr into cells expressing *slpr* (Fig. 8C and H). This modestly reduced JNK activity (measured by the intensity of *puc-lacZ*, see Section 2, Fig. 8C and E) and reduced *slpr*-induced cell migration (Fig. 8H). Indeed cell delamination and movement was not observed in 68% of $ptc > slpr$, *cindr*, *puc-lacZ* wing discs ($n=24$). We propose that in these wing epithelia ectopic Cindr partially corrected Cindr:$dJNK^{activated}$ stoichiometry to reduce JNK signaling.

4. Conclusions

Our finding that Cindr represses JNK activity to preserve epithelial integrity brings to light a role for this adaptor protein family that is likely of great importance in oncogenesis. Indeed the behavior of $cindr^{RNAi2}$-cells is akin to several established models of oncogenic-like cell migration that similarly utilize the *Drosophila* larval wing (Vidal et al., 2006; Singh et al., 2010; Vidal et al., 2010; Das et al., 2012; Rudrapatna et al., 2013; Dar et al., 2012; Cordero et al., 2010; Fernandez et al., 2014; Speck et al., 2003; Neisch et al., 2010). In these models, JNK activity mediated the migratory behavior of cells. Our data indicate that Cindr functions in a complex with *Drosophila* JNK to repress JNK signaling. Hence in the fly wing epithelium, Cindr functions as a tumor suppressor to repress oncogenic activity. The vertebrate orthologs Cd2ap and Cin85 have not yet been ascribed tumor suppressor activity, though their altered expression in a range of cancers has been reported (Bogler et al., 2000; Nam et al., 2007; Wakasaki et al., 2010; Ma et al., 2011; Mayevska et al., 2006) and genomics efforts have detected missense mutations in a small number of tumors, predominantly carcinomas (http://cancer.sanger.ac.ukcosmic). Hence the role and regulation of Cd2ap/Cin85 in these cancers requires further

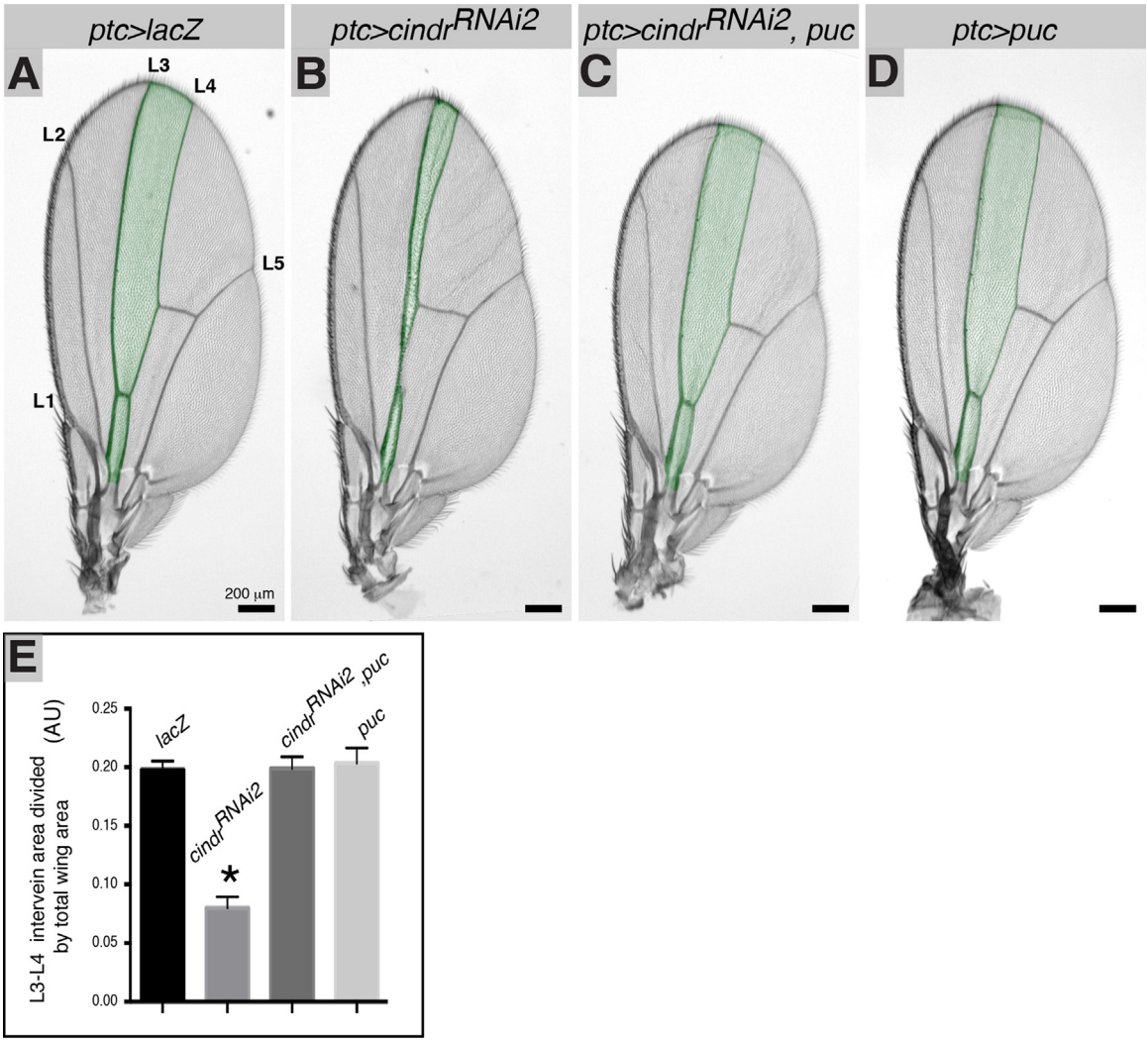

Fig. 7. Repressing JNK signaling rescued loss of tissue from *ptc > cindr*^{RNAi2} wings. (A–D) Representative *ptc > lacZ* (A), *ptc > cindr*^{RNAi2} (B), *ptc > cindr*^{RNAi2}, *puc* (C) and *ptc > puc* (D) adult wings. Green pseudocolor highlights the region between the L3 and L4 wing veins that corresponds to the *ptc*-expression domain. Anterior to the left, longitudinal veins are labeled L1–5. (D) Quantification of relative areas of the *ptc* domain indicated significant loss of tissue from *ptc > cindr*^{RNAi2} adult wings ($n=25$) when compared to control *ptc > lacZ* wings ($n=25$), but significant rescue when *puc* was co-expressed (*, $p < 0.0001$, $n=25$). The area between wing veins L3 and L4 was taken to represent the *ptc* domain. This area was normalized by division by the entire area of the wing blade. Error bars represent standard deviation.

investigation. Cindr and its orthologs may well also modulate JNK signaling in other contexts. For example, Cindr may regulate JNK to facilitate efficient healing of wounds and the appropriate morphogenesis of embryonic tissues.

We found the stoichiometry of Cindr-dJNK complexes to be crucial: even mild reduction of Cindr was sufficient to trigger some expression of JNK signaling targets. When Cindr was more severely reduced, JNK signaling was sufficiently activated to drive cells to constrict, delaminate, migrate and die. Occasionally, *cindr*^{RNAi2} cells were also observed traveling through the apical third of the wing epithelium. These phenotypes were remarkably well rescued in the presence of ectopic Puc, the dJNK phosphatase. This was surprising as Cindr (and its orthologs) has the capacity to assemble diverse protein complexes, yet our data suggested that Cindr-dJNK complexes dominate in the larval wing, where these are required to maintain the epithelium in a state of equilibrium appropriate for its correct development. Cindr's repression of dJNK is modeled in Fig. 9. We predict that we have uncovered a conserved mechanism that fine-tunes JNK activity and warrants investigation in other systems.

Given that Cindr limits JNK activity, two immediate questions come to mind. First, when cell migration is triggered in oncogenic-like *Drosophila* models, during wound healing, or during morphogenetic movements in the embryo, how is Cindr's repressive hold on JNK alleviated? We anticipate that a variety of strategies could be employed during these events. These include elevation of the concentration of activated JNK to disrupt Cindr-dJNK stoichiometry or direct modification of Cindr to disrupt its interaction with dJNK. Ectopic Rho1 activity, for example, which drives cell migration (Speck et al., 2003; Neisch et al., 2010), might elevate the concentration of activated dJNK to bypass the inhibitory effect of Cindr. Mammalian orthologs of Cindr appear to be targets of Src (Kirsch et al., 1999) and, in the fly wing, ectopic Src activity also drives cell movement (Vidal et al., 2006). We hypothesize that ectopic Src phosphorylates Cindr to modify the integrity or function of Cindr-dJNK complexes, triggering JNK activity. Expression of *cindr* may also be repressed to facilitate JNK activity. However, it turns out that the ortholog Cd2ap is a transcriptional target of Jun/Fos complexes when activated by Epidermal Growth Factor Receptor signaling *in vitro* (Lu et al., 2009). If *cindr* expression is also activated as a consequence of JNK signaling, this would provide a route for negative feedback that further fine-tunes JNK.

Second, our data raises the intriguing question: what mechanism is employed by Cindr to repress dJNK? We anticipate that

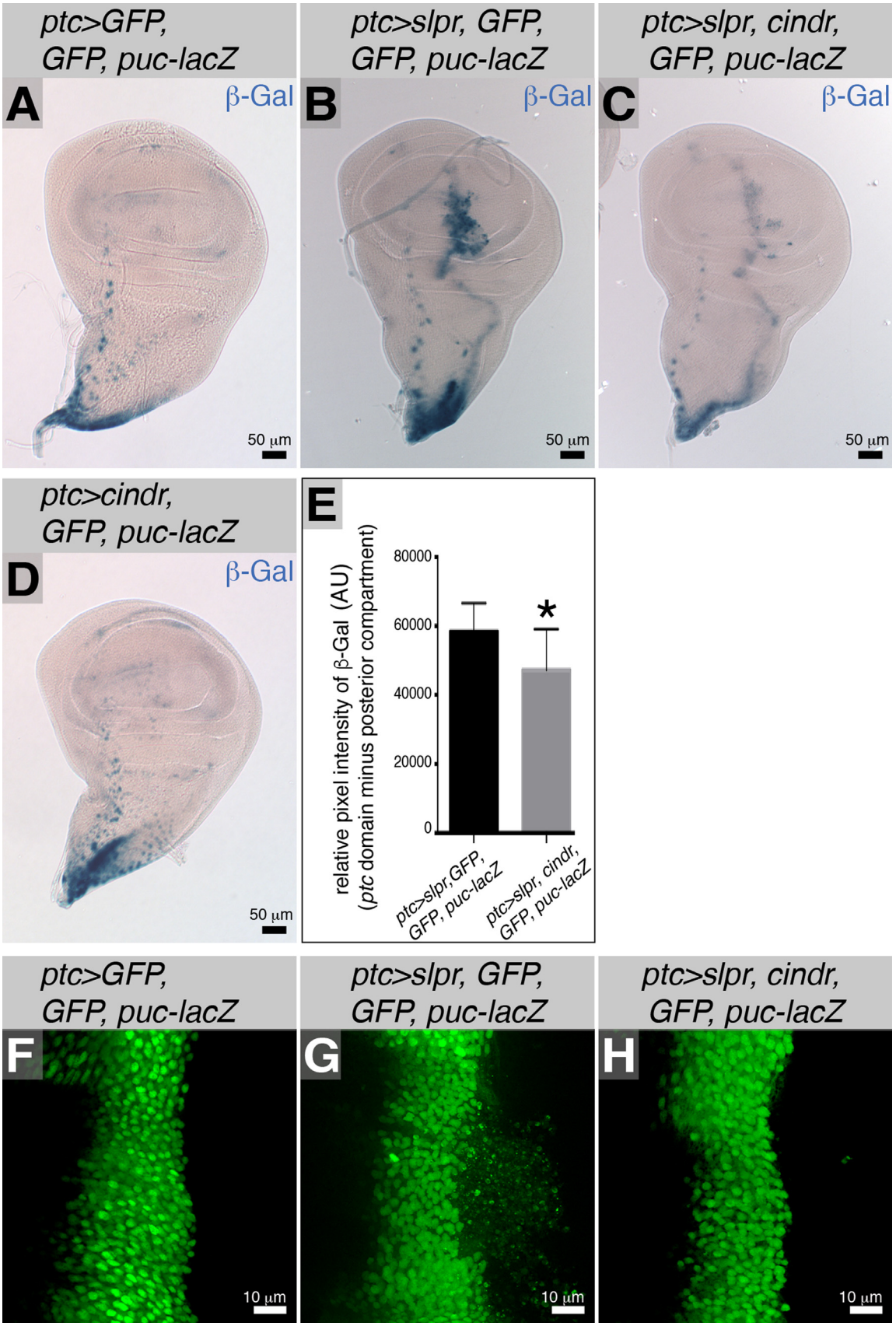

Fig. 8. Correct Cindr-dJNK stoichiometry was required to maintain epithelial integrity. (A) Wild type JNK activity (*puc-lacZ*-expression) was observed in *ptc > GFP*, *GFP*, *puc-lacZ* wing discs. (B) In *ptc > slpr*, *GFP*, *GFP*, *puc-lacZ* tissue JNK was activated through the *ptc*-domain which was disrupted, indicating extensive cell migration. (C) Co-expression of *cindr* reduced *slpr*-induced JNK activity. (D) Ectopic JNK activity was not detected in *ptc > cindr*, *GFP*, *puc-lacZ* wings. (E) Quantification of *puc-lacZ* expression in *ptc > slpr*, *GFP*, *GFP*, *puc-LacZ* ($n=20$) and *ptc > slpr*, *cindr*, *GFP*, *puc-LacZ* wing discs ($n=21$) confirmed that ectopic Cindr suppressed *slpr*-induced JNK activity (* significant at the 5% level, $p=0.0017$). Error bars represent standard deviation. AU, arbitrary units. (F–H) Expression of *slpr* triggered cell delamination and displacement (G) that was suppressed when *cindr* was co-expressed with *slpr* (H). Note that GMA was not expressed in these wing discs and the adherens junctions are hence not visible. Expression of two *GFP* transgenes (F) and *cindr* (not shown) did not disrupt wing epithelia.

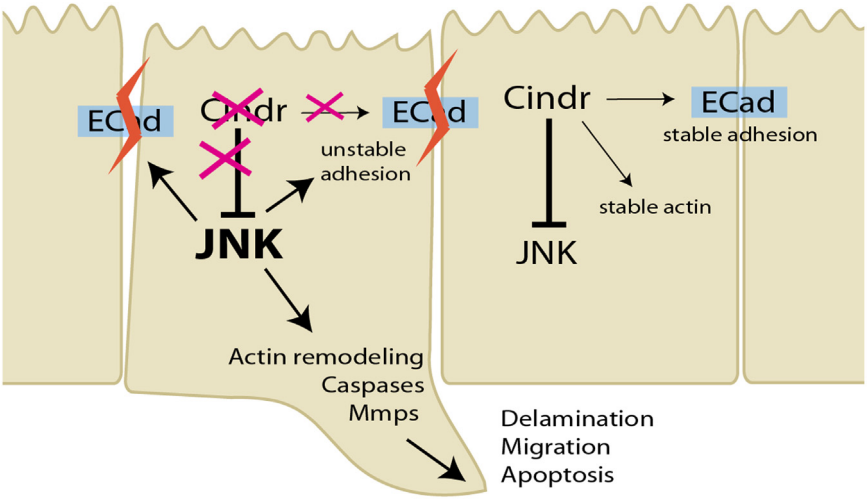

Fig. 9. Model of the relationship between Cindr and JNK signaling. Acting in a complex with dJNK, Cindr represses JNK signaling. Reducing Cindr releases the block on JNK signals that trigger remodeling of the actin cytoskeleton and production of MMPs that degrade extracellular matrix. Coupled with erosion of adhesion, cells are consequently released from stable positions within the epithelium and most cells delaminate. JNK activity also activates caspases that mediate death of delaminated cells. Also indicated in this model are functions of Cindr that stabilize the actin cytoskeleton and cell adhesion, independently of JNK. However our data indicated that in the wing epithelium Cindr functioned mainly through repression of JNK to maintain epithelial integrity.

Cindr could sequester dJNK from its target effectors or directly repress dJNK activity. For this latter possibility, we expect that effector proteins that mediate dJNK dephosphorylation or degradation could be recruited to Cindr-dJNK complexes. This suggestion highlights the important contributions that adaptor proteins play in assembling protein complexes that are crucial for the development, maintenance and function of epithelia. Indeed, our data illustrates that perturbing Cindr-dJNK complexes undermines tissue integrity, underscoring the importance of these proteins in developing and adult epithelia.

Acknowledgments

We thank numerous colleagues for donations of fly lines used in this study (listed in Experimental Procedures). In addition many stocks were obtained from the Bloomington Drosophila Stock Center (NIH P40OD018537). We thank Michael Weir, Stephen Devoto and Ross Cagan and his research team for constructive discussion and Laura Grabel and Michael Weir for feedback on this manuscript. Mark Hellerman provided invaluable technical support. This work was supported by Project Grants awarded to RIJ by Wesleyan University.

Appendix A. Supplementary material

Supplementary data associated with this article can be found in the online version at http://doi:10.1016/j.ydbio.2016.01.003.

References

Adler, V., Schaffer, A., Kim, J., Dolan, L., Ronai, Z., 1995. UV irradiation and heat shock mediate JNK activation via alternate pathways. J. Biol. Chem. 270 (44), 26071–26077 (Epub 1995/11/03. PubMed PMID: 7592807).

Adachi-Yamada, T., 2002. Puckered-GAL4 driving in JNK-active cells. Genesis 34 (1–2), 19–22. http://dx.doi.org/10.1002/gene.10110 (PubMed PMID: 12324941).

Bruck, S., Huber, T.B., Ingham, R.J., Kim, K., Niederstrasser, H., Allen, P.M., et al., 2006. Identification of a novel inhibitory actin-capping protein binding motif in CD2-associated protein. J. Biol. Chem. 281 (28), 19196–19203 (PubMed PMID: 16707503).

Baum, B., Georgiou, M., 2011. Dynamics of adherens junctions in epithelial establishment, maintenance, and remodeling. J. Cell Biol. 192 (6), 907–917. http://dx.doi.org/10.1083/jcb.201009141 (PubMed PMID: 21422226; PubMed Central PMCID: PMC3063136).

Baum, B., Settleman, J., Quinlan, M.P., 2008. Transitions between epithelial and mesenchymal states in development and disease. Semin. Cell Dev. Biol. 19 (3), 294–308. http://dx.doi.org/10.1016/j.semcdb.2008.02.001 (PubMed PMID: ISI:000255730600010).

Bogler, O., Furnari, F.B., Kindler-Roehrborn, A., Sykes, V.W., Yung, R., Huang, H.J., et al., 2000. SETA: a novel SH3 domain-containing adapter molecule associated with malignancy in astrocytes. Neuro Oncol. 2 (1), 6–15 (PubMed PMID: 11302255).

Chaffer, C.L., Weinberg, R.A., 2011. A perspective on cancer cell metastasis. Science 331 (6024), 1559–1564. http://dx.doi.org/10.1126/science.1203543 (PubMed PMID: 21436443).

Chatterjee, N., Bohmann, D., 2012. A versatile PhiC31 based reporter system for measuring AP-1 and Nrf2 signaling in Drosophila and in tissue culture. PLoS One 7 (4), e34063. http://dx.doi.org/10.1371/journal.pone.0034063 (PubMed PMID: 22509270; PubMed Central PMCID: PMC3324472).

Classen, A.K., Aigouy, B., Giangrande, A., Eaton, S., 2008. Imaging Drosophila pupal wing morphogenesis. Methods Mol. Biol. 420, 265–275. http://dx.doi.org/10.1007/978-1-59745-583-1_16 (PubMed PMID: 18641953).

Cai, D., Chen, S.C., Prasad, M., He, L., Wang, X., Choesmel-Cadamuro, V., et al., 2014. Mechanical feedback through E-cadherin promotes direction sensing during collective cell migration. Cell 157 (5), 1146–1159. http://dx.doi.org/10.1016/j.cell.2014.03.045 (PubMed PMID: 24855950; PubMed Central PMCID: PMC4118667).

Cordero, J.B., Macagno, J.P., Stefanatos, R.K., Strathdee, K.E., Cagan, R.L., Vidal, M., 2010. Oncogenic Ras diverts a host TNF tumor suppressor activity into tumor promoter. Dev. Cell 18 (6), 999–1011. http://dx.doi.org/10.1016/j.devcel.2010.05.014 (PubMed PMID: 20627081; PubMed Central PMCID: PMC3175220).

Dikic, I., 2002. CIN85/CMS family of adaptor molecules. FEBS Lett. 529 (1), 110–115 (PubMed PMID: 12354621).

Dikic, I., 2003. Mechanisms controlling EGF receptor endocytosis and degradation. Biochem. Soc. Trans. 31 (Pt. 6), 1178–1181 (PubMed PMID: 14641021).

Davis, R.J., 2000. Signal transduction by the JNK group of MAP kinases. Cell 103 (2), 239–252 (Epub 2000/11/01. PubMed PMID: 11057897).

Das, T.K., Sangodkar, J., Negre, N., Narla, G., Cagan, R.L., 2012. Sin3a acts through a multi-gene module to regulate invasion in Drosophila and human tumors. Oncogene 32 (26), 3184–3197. http://dx.doi.org/10.1038/onc.2012.326 (PubMed PMID: 22890320).

Dar, A.C., Das, T.K., Shokat, K.M., Cagan, R.L., 2012. Chemical genetic discovery of targets and anti-targets for cancer polypharmacology. Nature 486 (7401), 80–84. http://dx.doi.org/10.1038/nature11127 (PubMed PMID: 22678283).

Elbediwy, A., Zihni, C., Terry, S.J., Clark, P., Matter, K., Balda, M.S., 2012. Epithelial junction formation requires confinement of Cdc42 activity by a novel SH3BP1 complex. J. Cell Biol. 198 (4), 677–693. http://dx.doi.org/10.1083/jcb.201202094 (PubMed PMID: 22891260; PubMed Central PMCID: PMC3514035).

Eisenhoffer, G.T., Rosenblatt, J., 2013. Bringing balance by force: live cell extrusion controls epithelial cell numbers. Trends Cell Biol. 23 (4), 185–192. http://dx.doi.org/10.1016/j.tcb.2012.11.006 (PubMed PMID: 23273931; PubMed Central PMCID: PMC3615095).

Faul, C., Asanuma, K., Yanagida-Asanuma, E., Kim, K., Mundel, P., 2007. Actin up: regulation of podocyte structure and function by components of the actin cytoskeleton. Trends Cell Biol. 17 (9), 428–437 (PubMed PMID: 17804239).

Fanto, M., Weber, U., Strutt, D.I., Mlodzik, M., 2000. Nuclear signaling by Rac and

Rho GTPases is required in the establishment of epithelial planar polarity in the Drosophila eye. Curr. Biol. 10 (16), 979–988. http://dx.doi.org/10.1016/S0960-9822(00)00645-X (PubMed PMID: 10985385).
Fan, Y., Lee, T.V., Xu, D., Chen, Z., Lamblin, A.F., Steller, H., et al., 2010. Dual roles of Drosophila p53 in cell death and cell differentiation. Cell Death Differ. 17 (6), 912–921. http://dx.doi.org/10.1038/cdd.2009.182 (PubMed PMID: 19960025; PubMed Central PMCID: PMC3014827).
Fletcher, A.G., Osterfield, M., Baker, R.E., Shvartsman, S.Y., 2014. Vertex models of epithelial morphogenesis. Biophys. J. 106 (11), 2291–2304. http://dx.doi.org/10.1016/j.bpj.2013.11.4498 (PubMed PMID: 24896108; PubMed Central PMCID: PMCPMC4052277).
Fulga, T.A., Rorth, P., 2002. Invasive cell migration is initiated by guided growth of long cellular extensions. Nat. Cell Biol. 4 (9), 715–719. http://dx.doi.org/10.1038/ncb848 (PubMed PMID: 12198500).
Fernandez, B.G., Jezowska, B., Janody, F., 2014. Drosophila actin-Capping Protein limits JNK activation by the Src proto-oncogene. Oncogene 33 (16), 2027–2039. http://dx.doi.org/10.1038/onc.2013.155 (PubMed PMID: 23644660).
Garlena, R.A., Gonda, R.L., Green, A.B., Pileggi, R.M., Stronach, B., 2010. Regulation of mixed-lineage kinase activation in JNK-dependent morphogenesis. J. Cell Sci. 123 (Pt. 18), 3177–3188. http://dx.doi.org/10.1242/jcs.063313 (PubMed PMID: 20736302; PubMed Central PMCID: PMC2931609).
Garcia-Bellido, A., Ripoll, P., Morata, G., 1973. Developmental compartmentalisation of the wing disk of Drosophila. Nat. New Biol. 245 (147), 251–253 (PubMed PMID: 4518369).
Giot, L., Bader, J.S., Brouwer, C., Chaudhuri, A., Kuang, B., Li, Y., et al., 2003. A protein interaction map of Drosophila melanogaster. Science 302 (5651), 1727–1736. http://dx.doi.org/10.1126/science.1090289 (PubMed PMID: 14605208).
Halaoui, R., McCaffrey, L., 2015. Rewiring cell polarity signaling in cancer. Oncogene 34 (8), 939–950. http://dx.doi.org/10.1038/onc.2014.59 (PubMed PMID: 24632617).
Hanahan, D., Weinberg, R.A., 2011. Hallmarks of cancer: the next generation. Cell 144 (5), 646–674. http://dx.doi.org/10.1016/j.cell.2011.02.013 (PubMed PMID: 21376230).
Haglund, K., Nezis, I.P., Lemus, D., Grabbe, C., Wesche, J., Liestol, K., et al., 2010. Cindr interacts with anillin to control cytokinesis in Drosophila melanogaster. Curr. Biol. 20 (10), 944–950. http://dx.doi.org/10.1016/j.cub.2010.03.068 (PubMed PMID: 20451383).
Harris, T.J., Tepass, U., 2010. Adherens junctions: from molecules to morphogenesis. Nat. Rev. Mol. Cell Biol. 11 (7), 502–514. http://dx.doi.org/10.1038/nrm2927 (Epub 2010/06/24. PubMed PMID: 20571587).
Hay, B.A., Wolff, T., Rubin, G.M., 1994. Expression of baculovirus P35 prevents cell death in Drosophila. Development 120 (8), 2121–2129 (PubMed PMID: 7925015).
Igaki, T., Kanda, H., Yamamoto-Goto, Y., Kanuka, H., Kuranaga, E., Aigaki, T., et al., 2002. Eiger, a TNF superfamily ligand that triggers the Drosophila JNK pathway. EMBO J. 21 (12), 3009–3018. http://dx.doi.org/10.1093/emboj/cdf306 (PubMed PMID: 12065414; PubMed Central PMCID: PMC126061).
Johnson, R.I., Seppa, M.J., Cagan, R.L., 2008. The Drosophila CD2AP/CIN85 orthologue Cindr regulates junctions and cytoskeleton dynamics during tissue patterning. J. Cell Biol. 180 (6), 1191–1204 (PubMed PMID: 18362180).
Johnson, R.I., Sedgwick, A., D'Souza-Schorey, C., Cagan, R.L., 2011. Role for a Cindr-Arf6 axis in patterning emerging epithelia. Mol. Biol. Cell 22 (23), 4513–4526. http://dx.doi.org/10.1091/mbc.E11-04-0305 (PubMed PMID: 21976699; PubMed Central PMCID: PMC3226471).
Johnson, R.I., Bao, S., Cagan, R.L., 2012. Interactions between Drosophila IgCAM adhesion receptors and Cindr,the Cd2ap/Cin85 ortholog. Dev. Dyn. 241 (12), 1933–1943. http://dx.doi.org/10.1002/dvdy.23879, (PubMed PMID: 23027549).
Jasper, H., Benes, V., Schwager, C., Sauer, S., Clauder-Munster, S., Ansorge, W., et al., 2001. The genomic response of the Drosophila embryo to JNK signaling. Dev. Cell 1 (4), 579–586 (Epub 2001/11/13. PubMed PMID: 11703947).
Katoh, H., Fujita, Y., 2012. Epithelial homeostasis: elimination by live cell extrusion. Curr. Biol. 22 (11), R453–R455. http://dx.doi.org/10.1016/j.cub.2012.04.036 (PubMed PMID: 22677289).
Kirsch, K.H., Georgescu, M.M., Ishimaru, S., Hanafusa, H., 1999. CMS: an adapter molecule involved in cytoskeletal rearrangements. Proc. Natl. Acad. Sci. USA 96 (11), 6211–6216 (PubMed PMID: 10339567).
Lehtonen, S., Zhao, F., Lehtonen, E., 2002. CD2-associated protein directly interacts with the actin cytoskeleton. Am. J. Physiol. Ren. Physiol. 283 (4), F734–F743 (PubMed PMID: 12217865).
Lee, M.H., Koria, P., Qu, J., Andreadis, S.T., 2009. JNK phosphorylates beta-catenin and regulates adherens junctions. FASEB J. 23 (11), 3874–3883. http://dx.doi.org/10.1096/fj.08-117804 (PubMed PMID: 19667122; PubMed Central PMCID: PMC2774999).
Lee, M.H., Padmashali, R., Koria, P., Andreadis, S.T., 2011. JNK regulates binding of alpha-catenin to adherens junctions and cell-cell adhesion. FASEB J. 25 (2), 613–623. http://dx.doi.org/10.1096/fj.10-161380 (PubMed PMID: 21030692; PubMed Central PMCID: PMC3023394).
Lin, A., 2003. Activation of the JNK signaling pathway: breaking the brake on apoptosis. BioEssays: News Rev. Mol. Cell. Dev. Biol. 25 (1), 17–24. http://dx.doi.org/10.1002/bies.10204 (PubMed PMID: 12508278).
Liu, J., Lin, A., 2005. Role of JNK activation in apoptosis: a double-edged sword. Cell Res. 15 (1), 36–42. http://dx.doi.org/10.1038/sj.cr.7290262 (PubMed PMID: 15686625).
Lawrence, P.A., Struhl, G., 1996. Morphogens, compartments, and pattern: lessons from drosophila? Cell 85 (7), 951–961 (PubMed PMID: 8674123).
Landsberg, K.P., Farhadifar, R., Ranft, J., Umetsu, D., Widmann, T.J., Bittig, T., et al., 2009. Increased cell bond tension governs cell sorting at the Drosophila anteroposterior compartment boundary. Curr. Biol. 19 (22), 1950–1955. http://dx.doi.org/10.1016/j.cub.2009.10.021 (PubMed PMID: 19879142).
Lim, J., Thiery, J.P., 2012. Epithelial-mesenchymal transitions: insights from development. Development 139 (19), 3471–3486. http://dx.doi.org/10.1242/dev.071209 (PubMed PMID: 22949611).
Lu, C., Ren, W., Su, X.M., Chen, J.Q., Wu, S.H., Zhou, G.P., 2009. EGF-recruited JunD/c-fos complexes activate CD2AP gene promoter and suppress apoptosis in renal tubular epithelial cells. Gene 433 (1–2), 56–64. http://dx.doi.org/10.1016/j.gene.2008.11.015 (PubMed PMID: 19095050).
Martin-Belmonte, F., Perez-Moreno, M., 2012. Epithelial cell polarity, stem cells and cancer. Nat. Rev. Cancer 12 (1), 23–38. http://dx.doi.org/10.1038/nrc3169 (PubMed PMID: 22169974).
Mustonen, H., Lepisto, A., Lehtonen, S., Lehtonen, E., Puolakkainen, P., Kivilaakso, E., 2005. CD2AP contributes to cell migration and adhesion in cultured gastric epithelium. Biochem. Biophys. Res. Commun. 332 (2), 426–432 (PubMed PMID: 15910750).
Moreno, E., Yan, M., Basler, K., 2002. Evolution of TNF signaling mechanisms: JNK-dependent apoptosis triggered by Eiger, the Drosophila homolog of the TNF superfamily. Curr. Biol. 12 (14), 1263–1268 (Epub 2002/08/15. PubMed PMID: 12176339).
Marinari, E., Mehonic, A., Curran, S., Gale, J., Duke, T., Baum, B., 2012. Live-cell delamination counterbalances epithelial growth to limit tissue overcrowding. Nature 484 (7395), 542–545. http://dx.doi.org/10.1038/nature10984 (PubMed PMID: 22504180).
Muliyil, S., Krishnakumar, P., Narasimha, M., 2011. Spatial, temporal and molecular hierarchies in the link between death, delamination and dorsal closure. Development 138 (14), 3043–3054. http://dx.doi.org/10.1242/dev.060731 (PubMed PMID: 21693520).
Martin-Blanco, E., Gampel, A., Ring, J., Virdee, K., Kirov, N., Tolkovsky, A.M., et al., 1998. puckered encodes a phosphatase that mediates a feedback loop regulating JNK activity during dorsal closure in Drosophila. Genes Dev. 12 (4), 557–570 (Epub 1998/03/21. PubMed PMID: 9472024; PubMed Central PMCID: PMC316530).
Ma, Y., Ye, F., Xie, X., Zhou, C., Lu, W., 2011. Significance of PTPRZ1 and CIN85 expression in cervical carcinoma. Arch. Gynecol. Obstet. 284 (3), 699–704. http://dx.doi.org/10.1007/s00404-010-1693-9 (PubMed PMID: 20882291).
Mayevska, O., Shuvayeva, H., Igumentseva, N., Havrylov, S., Basaraba, O., Bobak, Y., et al., 2006. Expression of adaptor protein Ruk/CIN85 isoforms in cell lines of various tissue origins and human melanoma. Exp. Oncol. 28 (4), 275–281 (PubMed PMID: 17285110).
Naydenov, N.G., Hopkins, A.M., Ivanov, A.I., 2009. c-Jun N-terminal kinase mediates disassembly of apical junctions in model intestinal epithelia. Cell Cycle 8 (13), 2110–2121 (Epub 2009/06/09. PubMed PMID: 19502798).
Niewiadomska, P., Godt, D., Tepass, U., 1999. DE-Cadherin is required for intercellular motility during Drosophila oogenesis. J. Cell Biol. 144 (3), 533–547 (Epub 1999/02/11. PubMed PMID: 9971747; PubMed Central PMCID: PMC2132905).
Neisch, A.L., Speck, O., Stronach, B., Fehon, R.G., 2010. Rho1 regulates apoptosis via activation of the JNK signaling pathway at the plasma membrane. J. Cell Biol. 189 (2), 311–323. http://dx.doi.org/10.1083/jcb.200912010 (PubMed PMID: 20404112; PubMed Central PMCID: PMC2856900).
Nam, J.M., Onodera, Y., Mazaki, Y., Miyoshi, H., Hashimoto, S., Sabe, H., 2007. CIN85, a Cbl-interacting protein, is a component of AMAP1-mediated breast cancer invasion machinery. EMBO J. 26 (3), 647–656, (PubMed PMID: 17255943).
Picco, V., Pages, G., Linking, J.N.K., 2013. Activity to the DNA damage response. Genes Cancer 4 (9–10), 360–368. http://dx.doi.org/10.1177/1947601913486347 (PubMed PMID: 24349633; PubMed Central PMCID: PMC3863338).
Parisi, F., Vidal, M., 2011. Epithelial delamination and migration: lessons from Drosophila. Cell Adhes. Migr. 5 (4), 366–372 (Epub 2011/08/13. PubMed PMID: 21836393; PubMed Central PMCID: PMC3210305).
Rodriguez-Boulan, E., Macara, I.G., 2014. Organization and execution of the epithelial polarity programme. Nat. Rev. Mol. Cell Biol. 15 (4), 225–242. http://dx.doi.org/10.1038/nrm3775 (PubMed PMID: 24651541; PubMed Central PMCID: PMC4211427).
Rosette, C., Karin, M., 1996. Ultraviolet light and osmotic stress: activation of the JNK cascade through multiple growth factor and cytokine receptors. Science 274 (5290), 1194–1197 (Epub 1996/11/15. PubMed PMID: 8895468).
Ramet, M., Lanot, R., Zachary, D., Manfruelli, P., 2002. JNK signaling pathway is required for efficient wound healing in Drosophila. Dev. Biol. 241 (1), 145–156. http://dx.doi.org/10.1006/dbio.2001.0502 (PubMed PMID: 11784101).
Rios-Barrera, L.D., Riesgo-Escovar, J.R., 2013. Regulating cell morphogenesis: the Drosophila jun n-terminal kinase pathway. Genesis 51 (3), 147–162. http://dx.doi.org/10.1002/dvg.22354 (PubMed PMID: 23109363).
Repiso, A., Bergantinos, C., Corominas, M., Serras, F., 2011. Tissue repair and regeneration in Drosophila imaginal discs. Dev. Growth Differ. 53 (2), 177–185. http://dx.doi.org/10.1111/j.1440-169X.2010.01247.x (PubMed PMID: 21338344).
Roth, S., Stein, D., Nusslein-Volhard, C., 1989. A gradient of nuclear localization of the dorsal protein determines dorsoventral pattern in the Drosophila embryo. Cell 59 (6), 1189–1202 (Epub 1989/12/22. PubMed PMID: 2688897).
Rallis, A., Moore, C., Ng, J., 2010. Signal strength and signal duration define two distinct aspects of JNK-regulated axon stability. Dev. Biol. 339 (1), 65–77. http://dx.doi.org/10.1016/j.ydbio.2009.12.016 (PubMed PMID: 20035736; PubMed Central PMCID: PMC2845820).
Rudrapatna, V.A., Bangi, E., Cagan, R.L., 2014. A Jnk-Rho-Actin remodeling positive feedback network directs Src-driven invasion. Oncogene 33 (21), 2801–2886.

http://dx.doi.org/10.1038/onc.2013.232 (PubMed PMID: 23831567).
Stronach, B., 2005. Dissecting JNK signaling, one KKKinase at a time. Dev. Dyn. 232 (3), 575–584. http://dx.doi.org/10.1002/dvdy.20283 (PubMed PMID: 15704176).
Singh, J., Aaronson, S.A., Mlodzik, M., 2010. Drosophila Abelson kinase mediates cell invasion and proliferation through two distinct MAPK pathways. Oncogene 29 (28), 4033–4045. http://dx.doi.org/10.1038/onc.2010.155 (PubMed PMID: 20453880; PubMed Central PMCID: PMC2919309).
Speck, O., Hughes, S.C., Noren, N.K., Kulikauskas, R.M., Fehon, R.G., 2003. Moesin functions antagonistically to the Rho pathway to maintain epithelial integrity. Nature 421 (6918), 83–87. http://dx.doi.org/10.1038/nature01295 (PubMed PMID: 12511959).
Stanyon, C.A., Liu, G., Mangiola, B.A., Patel, N., Giot, L., Kuang, B., et al., 2004. A Drosophila protein-interaction map centered on cell-cycle regulators. Genome Biol. 5 (12), R96. http://dx.doi.org/10.1186/gb-2004-5-12-r96 (PubMed PMID: 15575970; PubMed Central PMCID: PMC545799).
Stronach, B., Perrimon, N., 2002. Activation of the JNK pathway during dorsal closure in Drosophila requires the mixed lineage kinase, slipper. Genes Dev. 16 (3), 377–387. http://dx.doi.org/10.1101/gad.953002 (PubMed PMID: 11825878; PubMed Central PMCID: PMC155330).
Tang, V.W., Brieher, W.M., 2013. FSGS3/CD2AP is a barbed-end capping protein that stabilizes actin and strengthens adherens junctions. J. Cell Biol. 203 (5), 815–833 (PubMed PMID: 24322428).
Tossidou, I., Teng, B., Drobot, L., Meyer-Schwesinger, C., Worthmann, K., Haller, H., et al., 2010. CIN85/RukL is a novel binding partner of nephrin and podocin and mediates slit diaphragm turnover in podocytes. J. Biol. Chem. 285 (33), 25285–25295. http://dx.doi.org/10.1074/jbc.M109.087239 (PubMed PMID: 20457601; PubMed Central PMCID: PMC2919091).
Vidal, M., Larson, D.E., Cagan, R.L., 2006. Csk-deficient boundary cells are eliminated from normal Drosophila epithelia by exclusion, migration, and apoptosis. Dev. Cell. 10 (1), 33–44 (PubMed PMID: 16399076).
Vidal, M., Salavaggione, L., Ylagan, L., Wilkins, M., Watson, M., Weilbaecher, K., et al., 2010. A role for the epithelial microenvironment at tumor boundaries: evidence from Drosophila and human squamous cell carcinomas. Am. J. Pathol. 176 (6), 3007–3014. http://dx.doi.org/10.2353/ajpath.2010.090253 (PubMed PMID: 20363916; PubMed Central PMCID: PMC2877860).
Weinberg, R.A., 2013. The Biology of Cancer, 2nd ed. Garland Science, NY.
Wogan, G.N., Hecht, S.S., Felton, J.S., Conney, A.H., Loeb, L.A., 2004. Environmental and chemical carcinogenesis. Semin. Cancer Biol. 14 (6), 473–486. http://dx.doi.org/10.1016/j.semcancer.2004.06.010 (PubMed PMID: 15489140).
Welsch, T., Endlich, N., Gokce, G., Doroshenko, E., Simpson, J.C., Kriz, W., et al., 2005. Association of CD2AP with dynamic actin on vesicles in podocytes. Am. J. Physiol. Ren. Physiol. 289 (5), F1134–F1143 (PubMed PMID: 15956777).
Wakasaki, T., Masuda, M., Niiro, H., Jabbarzadeh-Tabrizi, S., Noda, K., Taniyama, T., et al., 2010. A critical role of c-Cbl-interacting protein of 85 kDa in the development and progression of head and neck squamous cell carcinomas through the ras-ERK pathway. Neoplasia 12 (10), 789–796 (Epub 2010/10/12. PubMed PMID: 20927317; PubMed Central PMCID: PMC2950328).
Yaddanapudi, S., Altintas, M.M., Kistler, A.D., Fernandez, I., Moller, C.C., Wei, C., et al., 2011. CD2AP in mouse and human podocytes controls a proteolytic program that regulates cytoskeletal structure and cellular survival. J. Clin. Investig. 121 (10), 3965–3980. http://dx.doi.org/10.1172/JCI58552 (PubMed PMID: 21911934; PubMed Central PMCID: PMC3195478).
You, H., Lei, P., Andreadis, S.T., 2013. JNK is a novel regulator of intercellular adhesion. Tissue Barriers 1 (5), e26845. http://dx.doi.org/10.4161/tisb.26845 (PubMed PMID: 24868495; PubMed Central PMCID: PMC3942331).
Zhao, J., Bruck, S., Cemerski, S., Zhang, L., Butler, B., Dani, A., et al., 2013. CD2AP links cortactin and capping protein at the cell periphery to facilitate formation of lamellipodia. Mol. Cell. Biol. 33 (1), 38–47. http://dx.doi.org/10.1128/MCB.00734-12 (PubMed PMID: 23090967; PubMed Central PMCID: PMC3536300).